REPORT
232

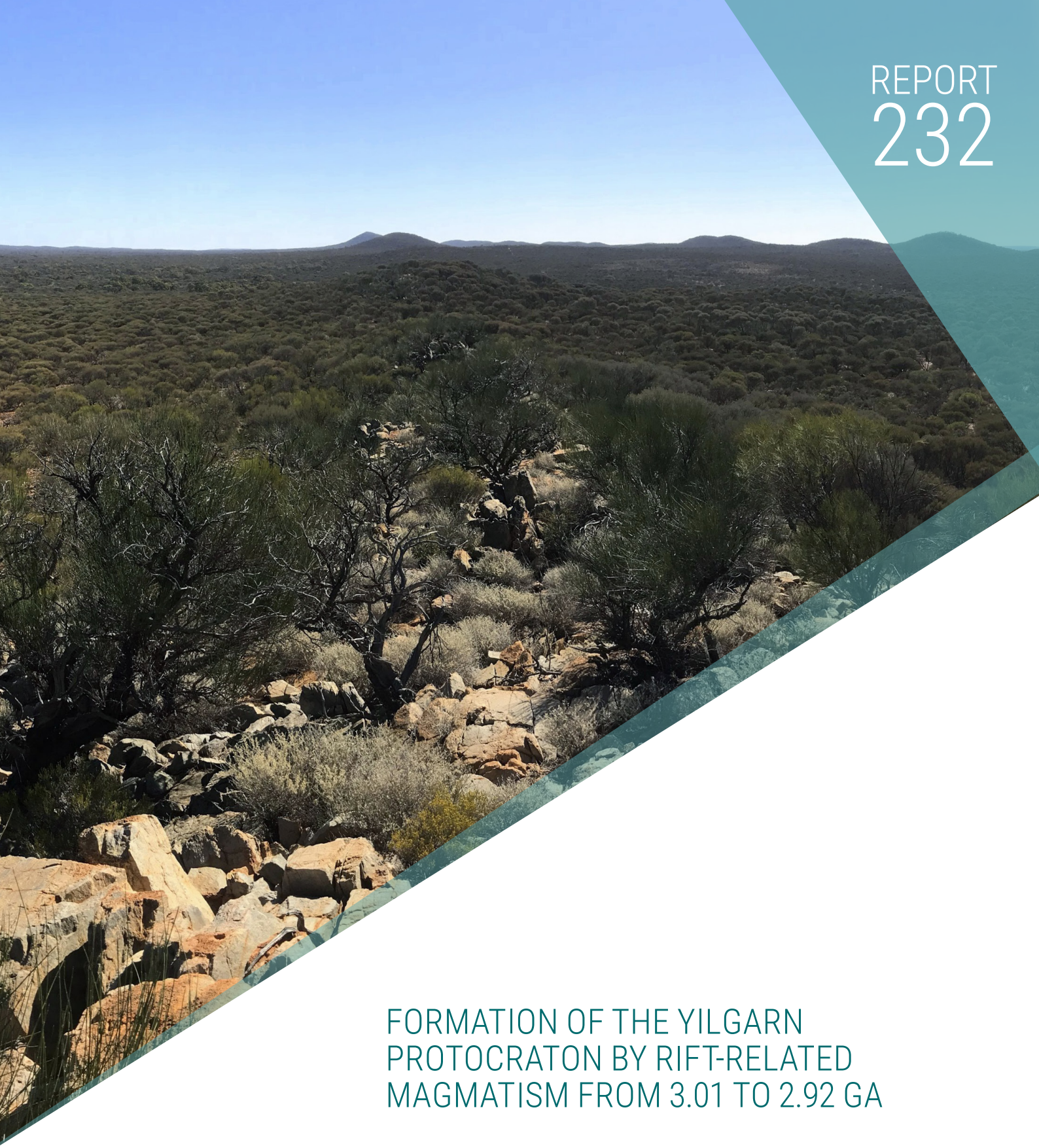

FORMATION OF THE YILGARN PROTOCRATON BY RIFT-RELATED MAGMATISM FROM 3.01 TO 2.92 GA

TJ Ivanic, MTD Wingate, JR Lowrey and Y Lu

Government of **Western Australia**
Department of **Mines, Industry Regulation and Safety**

Geological Survey of Western Australia

Government of **Western Australia**
Department of **Mines, Industry Regulation and Safety**

REPORT 232

FORMATION OF THE YILGARN PROTOCRATON BY RIFT-RELATED MAGMATISM FROM 3.01 TO 2.92 Ga

TJ Ivanic, MTD Wingate, JR Lowrey and Y Lu

PERTH 2022

Geological Survey of Western Australia

MINISTER FOR MINES AND PETROLEUM
Hon Bill Johnston MLA

DIRECTOR GENERAL, DEPARTMENT OF MINES, INDUSTRY REGULATION AND SAFETY
Richard Sellers

EXECUTIVE DIRECTOR, GEOLOGICAL SURVEY AND RESOURCE STRATEGY
Michele Spencer

REFERENCE
The recommended reference for this publication is:
Ivanic, TJ, Wingate, MTD, Lowrey, JR and Lu, Y 2022, Formation of the Yilgarn protocraton by rift-related magmatism from 3.01 to 2.92 Ga: Geological Survey of Western Australia, Report 232, 34p.

ISBN 978-1-74168-977-8
ISSN 1834-2280

A catalogue record for this book is available from the National Library of Australia

Grid references in this publication refer to the Geocentric Datum of Australia 1994 (GDA94). Locations mentioned in the text are referenced using Map Grid Australia (MGA) coordinates, Zone 50. All locations are quoted to at least the nearest 100 m.

U–Pb measurements were conducted using the SHRIMP II ion microprobes at the John de Laeter Centre, Curtin University, with financial support of the Australian Research Council and AuScope NCRIS.

Published 2022 by the Geological Survey of Western Australia
This Report is published in digital format (PDF) and is available online at <www.dmirs.wa.gov.au/GSWApublications>.

Further details of geoscience products are available from::
First Floor Counter
Department of Mines, Industry Regulation and Safety
100 Plain Street
EAST PERTH WESTERN AUSTRALIA 6004
Telephone: +61 8 9222 3459 Email: publications@dmirs.wa.gov.au
www.dmirs.wa.gov.au/GSWApublications

Cover photograph: Looking north from a ridge of quartzite within the Yalgoo–Singleton greenstone belt, western Youanmi Terrane

Contents

Figures

Tables

Appendices

Available with the PDF online as an accompanying digital resource

1. Whole-rock geochemistry data
2. Zircon U–Pb isotope data
3. Zircon Lu–Hf isotope data

Formation of the Yilgarn protocraton by rift-related magmatism from 3.01 to 2.92 Ga

TJ Ivanic, MTD Wingate, JR Lowrey and Y Lu

Abstract

The interpreted ages from new geochronology have allowed the definition of the ten stratigraphic, volcano-sedimentary associations and their grouping into the Southern Cross Supergroup. These associations yield magmatic crystallization ages between 3.01 and 2.92 Ga and are mapped in several belts along a 750 km long corridor within the Youanmi Terrane of the western Yilgarn Craton in Western Australia. These associations comprise six named formations and four other greenstone successions, which we combine into the Southern Cross Supergroup. Though not voluminous, the formations are locally well preserved in the stratigraphically lower portions of greenstone belts and are interpreted to unconformably underlie the c. 2.8 Ga Norie and Polelle Groups of the Murchison Supergroup. The Southern Cross Supergroup consists of equal parts basaltic and andesite–dacite–rhyolite rocks, and variable proportions of sedimentary rocks. In many areas, there are spatially associated synvolcanic tonalite–trondhjemite–granodiorite (TTG) plutons. Whole-rock geochemistry of felsic volcanic rocks indicates multiple source depths and locally highly fractionated compositions. High-Mg basaltic rocks of the Sandstone greenstone belt initially thought to represent a northerly extension of a c. 2.9 Ga komatiite succession at Ravensthorpe, are now reinterpreted as younger greenstone of the Polelle Group, thus the dominant trend of Southern Cross Supergroup is within a distinct, northwest-trending corridor from Ravensthorpe in the south to the Weld Range in the north. More widely distributed TTG gneisses in the Youanmi Terrane, with magmatic crystallization ages between 3.05 and 2.99 Ga, may have formed basement to the 3.01 – 2.91 Ga volcano-sedimentary rocks, as their chemical compositions are consistent with melting of lower-crustal sources. After deposition of the Southern Cross Supergroup, a magmatic hiatus occurred between 2.91 and 2.82 Ga. Zircon Lu–Hf data for two of the formations of the Southern Cross Supergroup and their proximal, synvolcanic TTGs yield a unimodal peak in εHf values spread over 40 Ma, with εHf indistinguishable from CHUR and with no indication of significant crustal contamination. Distal to the volcanic rocks of the Southern Cross Supergroup, TTG gneisses of the Thundelarra Supersuite are slightly more evolved, with εHf(i) between 0 and -2, indicating minor contributions from a >3.3 Ga crustal component. We consider the geometry of these formations, their homogeneous mantle source, and the punctuated chronology over 100 Ma to be consistent with a rift setting, in which the rift axis was coincident with the juvenile Cue Isotopic Zone (Sm–Nd T_{DM}^2 = 2.95 Ga) immediately to the east. Additional data may be needed to rule out other tectonic processes during this time interval. We consider the wide distribution of supracrustal rocks and TTGs from 3.01 to 2.91 Ga to represent a significant protocratonic stage and a significant building block of the Archean Yilgarn Craton.

KEYWORDS: Archean; geochronology; greenstone belts; hafnium isotopes; Mesoarchean; stratigraphy; volcanic-hosted massive sulfide; Yilgarn Craton

Introduction

The Youanmi Terrane has long been known to contain some of the older components of the Archean Yilgarn Craton (e.g. Gee, 1980). Establishing a stratigraphic–magmatic framework in such a long-lived portion of crust is essential in understanding the geodynamic history of such terranes and it relies heavily on wide coverage of geochronology samples in combination with field observations, geological mapping and other geological datasets. Until now, the stratigraphic–magmatic framework of the Youanmi Terrane, established by Van Kranendonk et al. (2013), provided in-depth coverage of the 2.82 – 2.7 Ga geological history but it lacked detail of the older rock units. Understanding these older units is essential to piece together the initial configuration of the Yilgarn Craton in its protocratonic state. The isotopic and geochemical features of these older crustal blocks can be used to infer potential processes that may have led to the formation of the Yilgarn protocraton. This knowledge may have significant implications for the geodynamics and mineral systems of both >2.82 Ga and <2.82 Ga rocks as older crustal boundaries are reactivated.

Several 3.01 – 2.92 Ga greenstone belts and TTG (tonalite–trondhjemite–granodiorite) gneiss units that extend for about 750 km in the 4 x 10^5 km^2 Youanmi Terrane share similarities in age and lithological characteristics (Fig. 1a,b). Supracrustal rocks in the greenstone belts can be grouped into six formations (the Gossan Hill, Mount Gibson, Madoonga, Honman, Wongan and Annabelle Volcanics Formations) and four unnamed greenstone successions. Though not voluminous, the formations are locally well-preserved and unconformably underlie the c. 2.8 Ga Norie and Polelle Groups of the Murchison Supergroup (Van Kranendonk et al., 2013). Most is known about the Gossan Hill Formation, which is located around the Golden Grove mine site in the western Youanmi Terrane (Fig. 2, inset), and dominated by felsic volcanic and volcaniclastic rocks. This formation hosts the second largest known Archean volcanogenic-hosted massive sulfide (VHMS) deposit, after Kidd Creek in the Abitibi sub-province, Canada, and therefore an understanding of rocks of this age is essential for mineral exploration. Although detailed knowledge of the lithological, mineralogical, metallurgical and structural aspects of parts of the Gossan Hill Formation is available, a wider appraisal

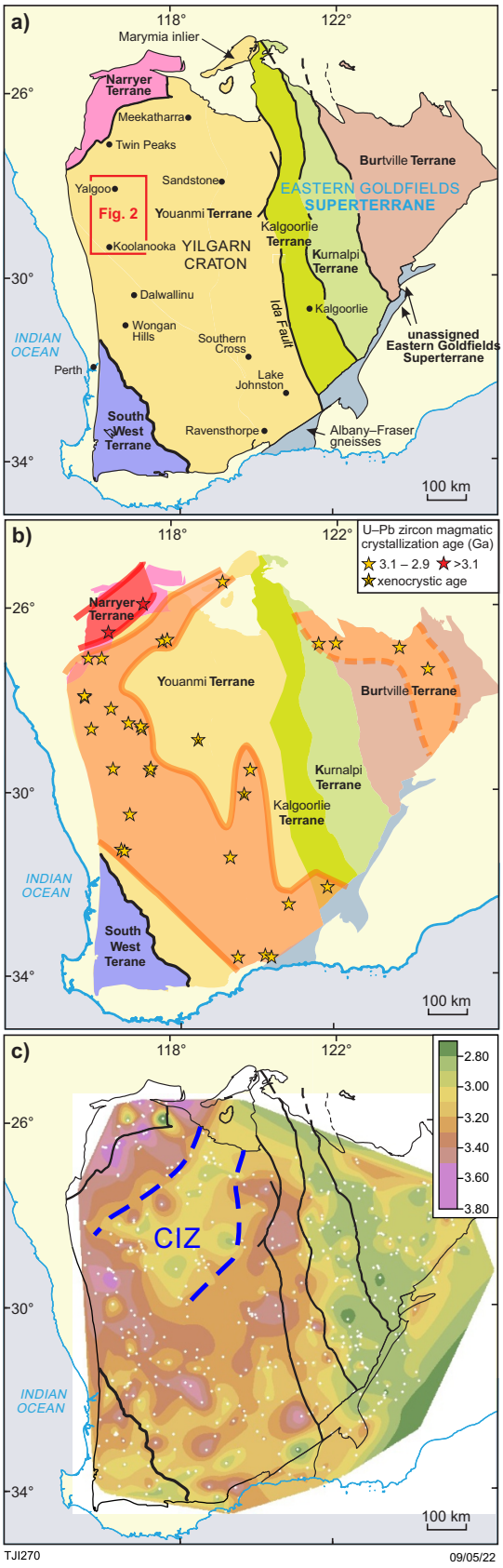

has been lacking and, until now, there has been no geological framework or understanding of the geodynamic setting for the formation of the isolated >2.9 Ga successions within the Youanmi Terrane.

Recent regional-scale mapping in the western Youanmi Terrane by the Geological Survey of Western Australia (GSWA) was informed by field relationships, geophysical and satellite imagery, geochronology, geochemistry and petrographic observations. This work has significantly improved our understanding of the regional geology, building on previous, detailed mine and mineral prospect-scale studies (e.g. Frater, 1983; Clifford, 1992; Yeats et al., 1996; Sharpe and Gemmel, 2001; 2002; Guilliamse, 2014). Initial aims of the regional mapping program were to use targeted geochronology and geochemistry to assign supracrustal rocks into formations and felsic and mafic plutonic rocks into suites.

Samples in this study augmented the density of Nd model-age locations in the Yilgarn-wide Sm–Nd isotope map (Fig. 1c; Lu et al., 2021). Eight U–Pb geochronology samples were selected for analysis of Hf isotopes in previously dated zircons to characterize the isotope ratios of the source region(s) from which magmas evolved. This may enable distinction between grains that have formed at the same time although with different ratios of crustal and mantle contributions.

In this report, we initially focus on the best-studied of these older formations, the Gossan Hill Formation (Golden Grove mine area), and we present an updated stratigraphic–magmatic scheme for rocks associated with the formation. With this basis, we expand by documenting the spatio-temporal framework for five other formations and four lithological associations. Altogether 13 samples were analysed for U–Pb zircon dating and eight of these were selected for Hf-in-zircon analysis. We relate the history of these units to key events in the development of the Youanmi Terrane (Van Kranendonk et al., 2013) and other 3.0 – 2.9 Ga magmatic events in the wider Yilgarn Craton. We describe the chemical variation within the Gossan Hill and Madoonga Formations. The discussion describes how our data are indicative of a craton-scale rift setting for this magmatism.

Figure 1. Yilgarn Craton maps: a) tectonic subdivisions (terrane boundaries after Cassidy et al. 2006), showing historically proposed terranes (red text) and selected domains (blue text). BaT = Ballingup Terrane, BoT = Boddington Terrane, LGT = Lake Grace Terrane, CT = Cocanarup Terrane, RT = Ravensthorpe Terrane, YT = Yamarna Terrane, SCD = Southern Cross Domain and MD = Murchison Domain; b) geochronology locations and distributions of 3.0–2.9 Ga and >3.0 Ga magmatic rocks. Hashed yellow-orange region highlights an area without known <2.9 Ga magmatic or sedimentary rocks. Dashed thick lines indicate boundaries of low confidence; c) contoured Sm–Nd two-stage depleted mantle model-age (T_{DM}^2) map showing sample locations as white dots and the outline of the redefined Cue Isotopic Zone (CIZ). Sm–Nd data are from latest compilation in Lu et al. (2021)

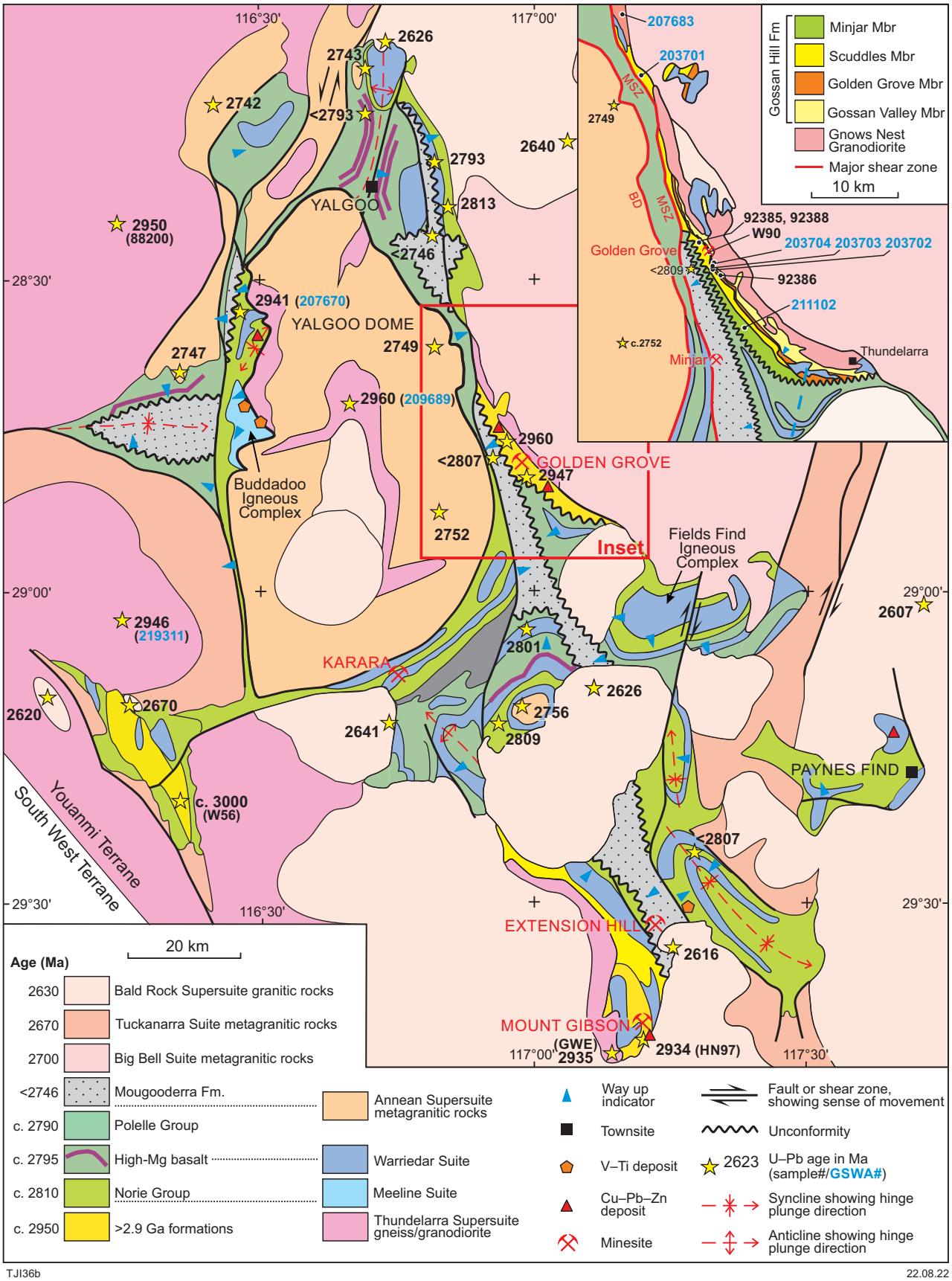

Figure 2. Simplified geological map of the Yalgoo–Singleton greenstone belt in the western Youanmi Terrane, including the Yalgoo Dome. Inset shows the Golden Grove area. Abbreviations: BD, Badja Decollement; MSZ, Mougooderra Shear Zone

Previous work

The western Youanmi Terrane was previously categorized as the 'Western Gneiss Province' (Gee, 1980), owing to its large proportion of orthogneiss. This region was thought to contain the oldest rocks of the Yilgarn Craton, including basement to the supracrustal greenstone successions. Several geochronological studies yielded ages between 3.01 and 2.92 Ga for rocks external to the Narryer Terrane, and included several felsic volcanic rocks dated at c. 2.95 Ga (e.g. Pidgeon et al., 1990; Pidgeon and Wilde, 1990; Nutman et al., 1993).

Previous workers have divided parts of the Yilgarn Craton into at least 12 terranes (including 22 domains). The southwestern Yilgarn Craton was divided into the Lake Grace, Boddington, and Ballingup Terranes (Wilde et al., 1996), and the Ravensthorpe greenstone belt in the southern Yilgarn Craton was divided into the Carlingup and Ravensthorpe Terranes and the Cocanarup greenstones (Witt, 1999). In the far eastern Yilgarn Craton, reassessment of zonation in isotopic ages led to excision of the Yamarna Terrane from the Burtville Terrane (Pawley et al. 2012). This terrane-dominated nomenclature is often used in conjunction with terrane-based models for crust generation via terrane assembly and/or arc accretion. Terrane boundaries have been correlated with structural discontinuities in seismic data (Wilde et al., 1996; Korsch et al., 2014). Korsch et al. (2014) also identified a similarity in seismic characteristics across the boundary between the Murchison and Southern Cross Domains and considered them as a single crustal entity, i.e. the Youanmi Terrane. These authors also attributed the differences in seismic character across the boundary between the Narryer and Youanmi Terranes to accretion between the two terranes. Cassidy et al. (2006) proposed the most recent terrane nomenclature for the Yilgarn Craton as a whole (Fig. 1a), although the South West/Youanmi Terrane boundary has been recently reinterpreted to lie approximately 200 km to the southwest of its previous location (Quentin de Gromard et al., 2021).

Between 1990 and 2015, GSWA conducted widespread mapping and geochronology studies in the western Youanmi Terrane, and eventually discovered additional 3.0 – 2.9 Ga gneissic rocks, including felsic volcanic units with ages of c. 2.95 Ga in various locations from Ravensthorpe in the south to the Weld Range in the north. The Annabelle Volcanics were mapped at Ravensthorpe (Witt, 1998), the Honman Formation at Lake Johnston (Wang et al., 1996; Romano et al., 2014), the Madoonga Formation at Weld Range (Wingate et al. 2008a), with further discoveries of c. 2.95 Ga volcanic rocks at Mount Gibson (Yeats et al., 1996), Gossan Hill (Pidgeon and Wilde, 1990), Tallering (Nutman et al., 1993) and Twin Peaks (Pidgeon and Wilde, 1990).

Ameen and Wilde (2018) used Hf isotopes and abundant 3.00 – 2.94 Ga xenocrystic zircons to infer multiple sources for, and prolonged reworking of, older granitic rocks in the Yalgoo area. They identified 3.85 to 3.00 Ga crustal reservoirs in the Yalgoo area that suggested the presence of Narryer Terrane material in basement of the western Youanmi Terrane (following Pidgeon and Hallberg, 2000; Cassidy et al., 2002; Wyche et al., 2004; Wyche 2007; Ivanic et al., 2012; Van Kranendonk et al., 2013).

Supracrustal rocks of the Youanmi Terrane were initially assigned to the Murchison Supergroup and divided into 'older' and 'younger' successions or associations (including several named formations), and periods at 3.0 Ga and 2.8 – 2.7 Ga were identified as significant periods of greenstone deposition (e.g. Watkins and Hickman, 1990; Pidgeon and Wilde, 1990; Pidgeon and Hallberg, 2000; Wang et al. 1998). Abundant granitic rocks were divided into several suites (Fig. 3) and later shown by geochronological relationships to parallel and complement the supracrustal evolution between 2.95 and 2.72 Ga (e.g. Yeats et al. 1996; Ivanic et al. 2012; Van Kranendonk et al. 2013). Furthermore, geochronological data from mafic–ultramafic rocks of the northern Youanmi Terrane (Ivanic et al., 2010; Ivanic, 2019) yielded four mafic–ultramafic intrusive suites dated between 2.81 and 2.72 Ga (Fig. 3). Hafnium isotope data for 2.98 – 2.60 Ga zircons from rocks in the northern Youanmi Terrane have provided a detailed evolution that included juvenile addition, crustal recycling, and/or magma mixing (Ivanic et al. 2012, 2013).

In the Yalgoo area, Clos et al. (2018) showed that the Yalgoo Dome contains large volumes of migmatitic rocks, including the c. 2.95 Ma Kynea Migmatite. These tonalitic rocks crosscut greenstones northwest of the dome in the Edamurta Range, indicating they are older than c. 2.951 Ga. Clos et al. (2018) invoked hydrous melting of mafic lower crust, but did not elucidate the geodynamic setting at c. 2.95 Ga. Zibra et al. (2020) proposed that protracted extension occurred after 2.95 Ga, forming basins into which subsequent supracrustal rocks were deposited.

Mole et al. (2014) classified Yilgarn Craton rocks in terms of their Hf isotope signatures. 'The Lake Johnston group', with intermediate εHf, located at the margin of negative (evolved) εHf signatures in the Hyden block, led the authors to interpret focused plume-driven magmatism at the paleo-craton margin. On a wider scale, Mole et al. (2019) showed an abundance of 3.00 – 2.91 Ga zircons in the Youanmi and Burtville Terranes, but rocks in this age range are also found sparsely within several other terranes. Mole et al. (2019) interpreted this zircon record to be a result of a major rifting event at c. 2.9 Ga in the southern Yilgarn Craton, with rift margins interpreted to trend east–west and northeast–southwest.

The Golden Grove area

The best-known formation older than 2.9 Ga in the Yilgarn Craton is the Gossan Hill Formation. The Golden Grove mine, currently owned by EMR Ltd, comprises underground and surface workings at Gossan Hill and Scuddles, located 4 km apart. Extensive mineralization was discovered at Gossan Hill in 1971 and at Scuddles in 1979. Scuddles underground operations began in 1990 and Gossan Hill underground operations started producing in 1998. Mining of copper oxide ore from an open pit at Gossan Hill commenced in early 2012 (MMG Golden Grove Pty Ltd; 2014). As of 30 June 2014, the total contained metals in all workings are Cu 0.7 Mt; Zn 1.3 Mt; Pb 0.1 Mt; Ag 42 Moz; Au 1.0 Moz (with an additional 5–30 % in estimated reserves) which, in terms of Archean VHMS deposits, makes it the largest in Australia and, globally, second only to the Kidd Creek deposit in Canada.

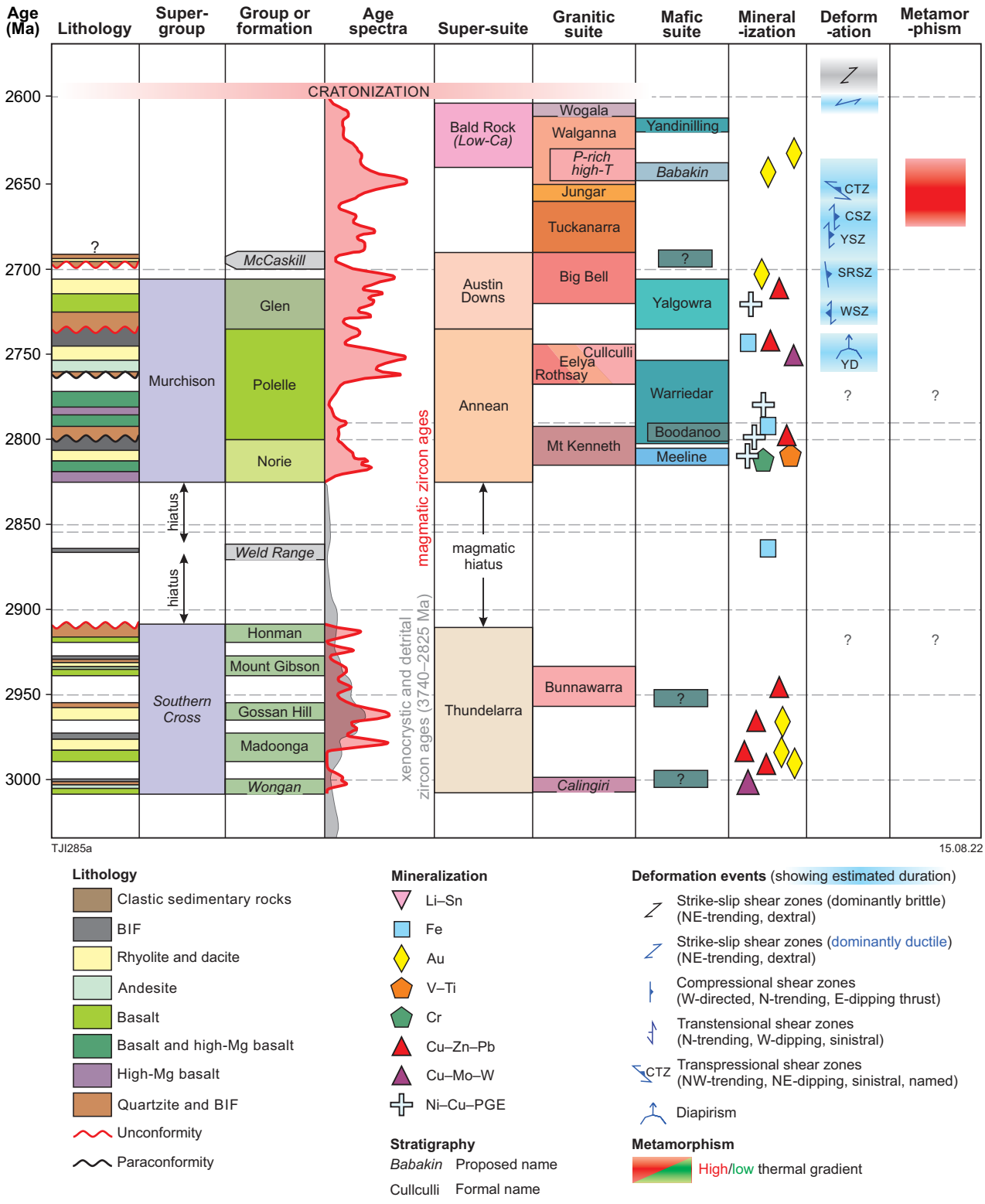

Figure 3. Updated stratigraphic framework for the Murchison and Southern Cross Supergroups showing relative probability curves for volcanic, plutonic and detrital zircon ages. Also shown are features of metamorphism deformation and mineralization. Italicized names are informal

Following the initial discovery, several studies describe the deposit in more detail (e.g. Frater, 1983). The first stratigraphic and volcanic assessment provided a lithostratigraphic model that divided the Golden Grove succession into several formations (Clifford, 1992). Further work, describing mineralization and alteration (Sharpe and Gemmel 2001; 2002), concluded that mineralization at the Gossan Hill deposit formed from a low-temperature seawater convection–alteration system, on which was superimposed a hotter mineralizing fluid that deposited massive magnetite and sulfide minerals along a synvolcanic feeder structure. Subsequent workers have utilized the stratigraphic scheme of Clifford (1992) and are in general agreement with the interpretation of a westerly way-up direction and a subaqueous felsic volcanic and volcaniclastic setting.

In terms of geochronological data, initial thermal ionization mass spectrometry (TIMS) analyses of few zircon crystals yielded c. 2940 Ma ages (Pidgeon and Wilde, 1990; Pidgeon, 1994). Sensitive High-Resolution Ion Microprobe (SHRIMP) analyses of numerous zircons from samples above and below the main mineralization at Gossan Hill yielded ages of c. 2960 Ma (Wang, 1998; Wang et al., 1998) as well as one date of c. 2945 Ma from the Scuddles Member. Table 1 shows how successive geochronological studies have required modifications to the stratigraphic scheme at Golden Grove.

Based on similarities in isotopic age, Guilliamse (2014) directly correlated felsic volcanic rocks at the Glenview prospect in the Weld Range (200 km north of Golden Grove) with those at Golden Grove. Geochemical data from these two areas were interpreted to indicate an active continental arc tectonic setting (Guilliamse, 2014; with Frater, 1983, also postulating an 'active tectonic environment' for the Golden Grove succession). Hollis et al. (2015) presented lithogeochemical data for volcanic rocks associated with VHMS occurrences in the Yilgarn Craton and showed that rhyolites with both enriched HREE (Heavy Rare Earth Elements) and low HREE compositions are present in the Golden Grove and the Scuddles Members. All these rocks plot in the FIIIa-type prospectivity field (Guilliamse, 2014; after Lesher et al., 1986).

Geological setting

Each of the ten 3.1 – 2.9 Ga successions (Fig. 4b and Table 2) contain 20–80% felsic volcanic rocks, interlayered with sedimentary rocks (Fig. 4a). There is a clear, typically interlayered, association of felsic volcanic rocks with intermediate and mafic volcanic rocks in most successions, and there are several occurrences of synvolcanic tonalite–granodiorite plutons. Although the Roundtop Komatiite and the Bandalup Ultramafics (in the Ravensthorpe greenstone belt) overlie 2.95 – 2.92 Ga felsic volcanic rocks, neither formation is demonstrably coeval with these older successions (Fig. 4, blue brackets). Furthermore, several dates at c. 2876, 2787 and 2720 Ma (Romano et al., 2014; Kennedy and Lane, 2001) in the Lake Johnston and Ravensthorpe greenstone belts indicate that many of the contained units are younger than 2.9 Ga (e.g. Romano et al., 2014), with subordinate, isolated units directly dated at 2.99 – 2.92 Ga (e.g. the Annabelle Volcanics). Thus, these older components, within the southern greenstone belts of the Youanmi Terrane, occur within younger greenstone packages, in a similar manner to those in the northwest Youanmi Terrane, such as the Gossan Hill Formation.

The 2.82 – 2.70 Ga Norie, Polelle and Glen Groups overlie the 3.0 – 2.9 Ga successions above either unconformable or sheared contacts (Fig. 4). The way-up of the ten successions is mostly known, although facing directions are sparse in the Tallering, Edamurta, Twin Peaks, Mount Gibson and Koolanooka greenstone belts. Way-up was inferred from graded bedding, cross-bedding, igneous differentiation in mafic–ultramafic sills, or flows and pillow structures in mafic volcanic rocks. The Madoonga Formation is the only succession to show a clear progression in basalt–andesite–rhyolite fractionation (e.g. Guilliamse, 2014). Mafic–ultramafic intrusions are present in most successions, although they are mostly not dated and are unassigned. Some of these mafic–ultramafic intrusions in the Yalgoo area are assigned to the c. 2.8 Ga Warriedar Suite (Fig. 2). The greenstone belts are transected by numerous faults and greenschist to upper amphibolite facies shear zones. Basal supracrustal contacts are typically truncated by shear zones or intruded by <2.8 Ga granitic gneiss and metagranodiorite (Ivanic et al., 2012) or intruded by post-tectonic plutons of the 2.65 – 2.60 Ga Bald Rock Supersuite (Fig. 4). In most greenstone belts, the stratigraphy is deformed into generally synformal folds up to 20 km in scale (e.g. Fig. 2). Some of this deformation has been linked to vertical tectonic movements in and around c. 2.75 Ga granitic domes such as the Yalgoo Dome (e.g. Zibra et al., 2020).

There are many smaller greenstone fragments and rafts within gneisses across the Youanmi Terrane that remain unassigned and undated. Although the 3.01 – 2.92 Ga units in the Youanmi Terrane share similarities across several greenstone belts, they cannot be petrologically or geochemically distinguished from rocks of the Polelle or Norie Groups without geochronological control. Thus, further work is required to establish the complete extents of these units.

Geological setting of the Golden Grove area

New mapping by GSWA in the Golden Grove area has especially helped to define aspects of the rocks associated with the Gossan Hill Formation and these rocks provide a basis for further study of c. 2.95 Ga rocks of the Youanmi Terrane. The four members of the Gossan Hill Formation (Table 1, Fig. 2, Fig. 4) are, in total, about three km thick, and consist of volcanic and volcaniclastic rocks, within which bedding is right way-up and steeply southwest-dipping. The formation is mapped in a 50 km long, north-northwest-trending, arcuate region up to 3.5 km wide, located on the eastern side of the Yalgoo–Singleton greenstone belt (Fig. 2), about 50 km southeast of Yalgoo.

To the north of the Golden Grove mine area, the succession becomes thinner, and the Gossan Valley and Golden Grove Members pinch out for about 7 km (Fig. 2, inset). The Minjar Member is truncated to the west by the Mougooderra Shear Zone in this area as well. The Scuddles Member does not thin to the north, but instead is gradually, and eventually entirely, truncated by the Mougooderra Shear Zone to the west and intruded by the Gnows Nest Granodiorite to the east. About six kilometres to the north-northwest of this point, along the Mougooderra Shear Zone, the Scuddles Member occupies a second, lens-shaped region about 5.8 km long.

Table 1. Previous and updated stratigraphic schemes for the Golden Grove succession

Watkins and Hickman (1990)	*Sharpe and Gemmell (2001) following Clifford (1992) for rocks of the Golden Grove Domain part of Gabanintha Formation*				*Mine sequence*	*Lithologies*	*Updated stratigraphy (this report)*			*Geochronology (ages in Ma)*							*Updated lithologies*
Formation	*Group*	*Total thickness (m)*	*Child units*	*Total thickness (m)*	*'members'*	*Previous description*	*Group*	*Formation*	*Member*	*Sample ID*	*Wang et al. (1998)*	*Sample ID*	*Pidgeon and Wilde (1990)*	*Sample ID*	*Pidgeon (1994)*	*Sample ID*	*This report*	*New description*
Windaning Formation						Felsic volcanogenic sedimentary rock (Wang, 1998)	Glen Group	Mougooderra Formation	unassigned	92382	<2809 ± 5					211101	<2746 ± 4	Siliciclastic, fining upward, elongate basin; chert pebble conglomerate, sandstone, siltstone, minor BIF, felsic volcanogenic rocks
UNCONFORMITY IDENTIFIED	UNCONFORMITY	U/C	UNCONFORMITY	U/C		UNCONFORMITY	UNCONFORMITY									UNCONFORMITY		unchanged
Gabanintha Formation	*Minjar Group*	>3700				Pillow basalts	Polelle Group	unassigned	unassigned								c. 2790	Pillow basalt; lesser BIF intruded by gabbro–pyroxenite
	Thundelarra Group	2300–2800	includes: *Pincers member*			Tholeiitic basalts; includes *'Pincers intermediate volcanics'*	Polelle Group	unassigned	unassigned								c. 2790	Tholeiitic basalt; lesser BIF intruded by gabbro–pyroxenite
Gabanintha Formation							CRYPTIC UNCONFORMITY									UNCONFORMITY		Geophysical interpretation and inferred from truncation of mapped trends
	Gossan Hill Group	2800–3100	*Cattle Well Formation (upper)*	900–1450		Andesitic volcanic rocks and greywackes			Minjar Member							211102	2947 ± 4	Felsic volcanic and volcaniclastic rocks, siltstone, amygdaloidal basalt, intruded locally by tonalite and gabbro
			Scuddles Formation	730–990	*SC4*	Dacite and rhyodacite feldspar-phyric intrusive and extrusive rocks			Scuddles Member				1			203702; 203701	2962 ± 4; 2958 ± 6	unchanged
					SC3	Tuff, breccia, chert, BIF, sulfides												unchanged
					SC2	Rhyodacite lava and breccia, massive dacite, sulfides				92385	2945 ± 4							unchanged
					SC1	Amygdaloidal dacite lava and breccia, minor sedimentary rocks		Gossan Hill Formation						unnamed	2951**			unchanged
			Golden Grove Formation	75–800	*GG6*	Bedded sandstone, siltstone, chert, sulfides			Golden Grove Member	92388	2960 ± 6							unchanged
					GG5	Lithic sandstone, pebble breccia, sulfides												unchanged
					GG4	Volcaniclastic pebble breccia, sulfides												unchanged
					GG3	Dacitic volcaniclastic rocks												unchanged
					GG2	Mixed siliciclastic and volcaniclastic rocks, andesite–dacite–rhyodacite lava										203703	2963 ± 6	unchanged
					GG1	Quartz-rich pumiceous pebble breccia, sandstone, dacite lava												unchanged
			Gossan Valley Formation (lower)	~3000	*GV4*	Sandstone to cobble breccia, minor basalt flows			Gossan Valley Member									unchanged
					GV3	Quartz- and feldspar-phyric rhyolite lava				92386	2953 ± 7	W90	2938 ± 10	W90	2957**	203704	2959 ± 5	unchanged
					GV2	Tuffaceous volcaniclastic breccia												unchanged
					GV1	Sandstone–pelitic rocks–breccia, minor basalt flows												**unchanged**
			Shadow Well Formation	150–1100		Arkose and quartz sandstone	Thundelarra Supersuite	Gnows Nest Granodiorite								**207683**	**2951 ± 6**	Metagranodiorite; typically schistose; locally deeply weathered

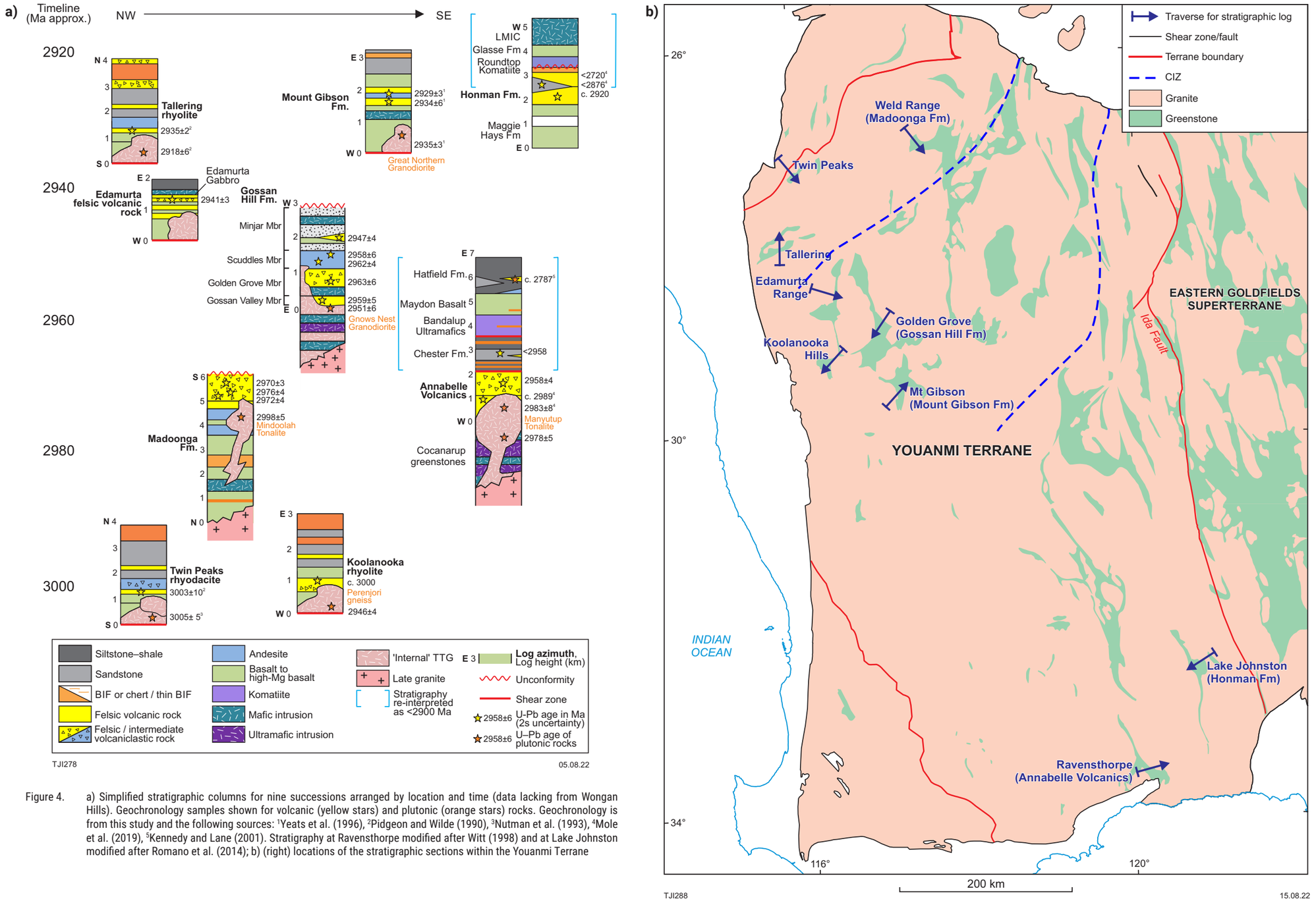

Figure 4. a) Simplified stratigraphic columns for nine successions arranged by location and time (data lacking from Wongan Hills). Geochronology samples shown for volcanic (yellow stars) and plutonic (orange stars) rocks. Geochronology is from this study and the following sources: [1]Yeats et al. (1996), [2]Pidgeon and Wilde (1990), [3]Nutman et al. (1993), [4]Mole et al. (2019), [5]Kennedy and Lane (2001). Stratigraphy at Ravensthorpe modified after Witt (1998) and at Lake Johnston modified after Romano et al. (2014); b) (right) locations of the stratigraphic sections within the Youanmi Terrane

Table 2. Compilation of 3.01 – 2.92 Ga isotopic ages in the Yilgarn Craton

Location (deposit)	*Stratigraphic name*	*Lithology*	*Sample ID*	*Age (Ma)*	*95% uncertainty (Ma)*	*Reference*	*Comment*
HONMAN FORMATION							
Lake Johnston (Maggie Hays)	Honman Formation	felsic volcanic rock	92-247	2903	5	Wang et al. (1996)	
Lake Johnston (Maggie Hays)	Honman Formation	felsic metavolcanic rock	207514	2916	4	Wingate et al. (2017a)	
Lake Johnston (Maggie Hays)	Honman Formation	rhyolite	LJD-0017-222	2920	4	Romano et al. (2014)	
Lake Johnston (Maggie Hays)	Honman Formation	felsic metavolcanic rock	207517	2921	4	Wingate et al. (2017b)	
Lake Johnston (Maggie Hays)	Honman Formation	dacite	92-246	2921	4	Wang et al. (1996)	
Lake Johnston	Honman Formation	felsic metavolcanic rock	199046	2922	4	Romano et al. (2014)	
Lake Johnston (Maggie Hays)	Honman Formation	felsic metavolcanic rock	207513	2924	6	Wingate et al. (2017c)	
MOUNT GIBSON FORMATION							
Mount Gibson (Orion 2)	Mount Gibson Formation	quartz porphyry	OR77	2929	3	Yeats et al. (1996)	
Mount Gibson	Thundelarra Supersuite	metagranodiorite	GWE	2935	7	Yeats et al. (1996)	
Mount Gibson	Thundelarra Supersuite	metagranodiorite	242405	2928	5	**Wingate et al. (2021a)**	**described in this study**
Mount Gibson (north)	**Mount Gibson Formation**	**metadacite**	**242407**	2932	5	**Wingate et al. (2021b)**	**described in this study**
Mount Gibson (Hornet)	Mount Gibson Formation	felsic schist	HN97	2934	6	Yeats et al. (1996)	
TALLERING FELSIC MAGMATIC ROCKS							
Tallering	unassigned	rhyodacite	W116	2935	2	Pidgeon and Wilde (1990)	multi-grain IDTIMS
EDAMURTA RANGE FELSIC VOLCANIC ROCKS							
Edamurta Range	**unassigned**	**felsic metavolcaniclastic rock**	**207670**	2941	3	Wingate et al. (2019)	**described in this study**
Edamurta Range	**unassigned**	**metagranodiorite**	**227224**	2941	3	Wingate et al. (2021c)	**described in this study**
GOSSAN HILL FORMATION							
Golden Grove	**Gnows Nest Granodiorite, Thundelarra Supersuite**	**metatonalite**	**207683**	2951	6	Lu et al. (2018)	**described in this study**
Golden Grove	**Minjar Member**	**felsic volcaniclastic rock**	**211102**	2947	4	Lu et al. (2016)	**described in this study; maximum depositional age**
Golden Grove	Scuddles Member	dacite	92382	2945	4	Wang et al. (1998)	
Golden Grove	Scuddles Member	dacite	(single zircon)	2951	-	Pidgeon et al. (1994)	
Golden Grove (north)	Scuddles Member	metadacite	203701	2958	6	**Lu et al. (2018)**	**described in this study**
Golden Grove	**Scuddles Member**	**metadacite**	**203702**	2962	2	**Wingate et al. (2015a)**	**described in this study**
Golden Grove	**Golden Grove Member**	**rhyolite**	**92385**	2960	6	Wang et al. (1998a)	
Golden Grove	Golden Grove Member	metarhyolite	203703	2963	6	**Wingate et al. (2015b)**	**described in this study**
Golden Grove	**Gossan Valley Member**	**rhyolite**	**92388**	2953	7	Wang et al. (1998a)	
Golden Grove	Gossan Valley Member	rhyolite	W90	2957	-	Pidgeon et al. (1994)	
Golden Grove	Gossan Valley Member	rhyolite	W90	2938	6	**Pidgeon and Wilde (1990)**	multi-grain IDTIMS – age based on oldest 3 analyses <5% discordant
Golden Grove	**Gossan Valley Member**	**metarhyolite**	**203704**	2959	5	**Wingate et al. (2015c)**	**described in this study**
RAVENSTHORPE FELSIC MAGMATIC ROCKS							
Ravensthorpe	Annabelle Volcanics	rhyolite	112163	2958	4	Nelson (1995a)	
Ravensthorpe	Annabelle Volcanics	quartzite	207506	2958	4	Wingate et al. (2017d)	maximum age of deposition
Ravensthorpe	Manyutup Tonalite	metatonalite	207510	2985	4	Wingate et al. (2018a)	
Ravensthorpe	Manyutup Tonalite	tonalite	ARC94	2983	8	Mole et al. (2019)	
Ravensthorpe	Annabelle Volcanics	rhyolite	ARC92A	2988	10	Mole et al. (2019)	
Ravensthorpe	Annabelle Volcanics	rhyolite	ARC95	2990	9	Mole et al. (2019)	
MADOONGA FORMATION							
Weld Range	Madoonga Formation	metasandstone	184112	2969	3	Wingate et al. (2008a)	maximum age of deposition
Weld Range	Madoonga Formation	felsic metavolcanic breccia	198240	2972	4	Wingate et al. (2015b)	
Weld Range	Madoonga Formation	felsic volcanic rock	96663	2976	4	Wang (1998)	
Weld Range	Madoonga Formation	metarhyolite	155569	2977	3	Wingate et al. (2013)	

Table 2. (continued)

Location (deposit)	*Stratigraphic name*	*Lithology*	*Sample ID*	*Age (Ma)*	*95% uncertainty (Ma)*	*Reference*	*Comment*
Weld Range	Madoonga Formation	metarhyolite clast	193972	2979	3	Wingate et al. (2012b)	
Weld Range	Mindoolah Tonalite	felsic schist (possibly meta-tonalite)	W50	c. 3 Ga	–	Pidgeon and Wilde (1990)	discordant multi-grain IDTIMS
KOOLANOOKA HILLS FELSIC MAGMATIC ROCKS							
Koolanooka Hills	**Thundelarra Supersuite**	**metamonzogranite**	219311	2946	4	**Wingate et al. (2020)**	**described in this study**
Koolanooka Hills	**unassigned**	**metavolcanic rock**	**242652**	2961	4	**Wingate et al. (2021b)**	**described in this study**
Koolanooka Hills	unassigned	rhyolite	W56	c. 3 Ga	–	Pidgeon and Wilde (1990)	multi-grain IDTIMS, 20–30% discordant
Koolanooka Hills	**unassigned**	**felsic metavolcanic rock**	**242672**	3002	4	**Wingate et al. (2021c)**	**described in this study**
TWIN PEAKS FELSIC MAGMATIC ROCKS							
Twin Peaks	unassigned	granitic gneiss	88169	3003	10	Pidgeon et al. (1990)	
Twin Peaks	unassigned	felsic volcanic rock	W78	3014	13	Pidgeon and Wilde (1990)	multi-grain IDTIMS, age based on one concordant analysis
WONGAN HILLS FELSIC MAGMATIC ROCKS							
Wongan Hills	unassigned	granitic gneiss	W7	c. 3 Ga	–	Pidgeon et al. (1990)	
Dalwallinu	unassigned	granitic gneiss	99969093B	3007	3	Fletcher and McNaughton (2002)	
Wongan Hills	unassigned	monzogranite gneiss	205930	3010	4	Wingate et al. (2018b)	
Wongan Hills	unassigned	syenogranite gneiss	205931	3010	4	Wingate et al. (2018c)	
Wongan Hills	unassigned	felsic porphyry	W1	3010	7	Pidgeon et al. (1990)	
Calingiri	Thundelarra Supersuite	granitic gneiss	224760	3018	4	Wingate et al. (2021)	
PROXIMAL GNEISSES							
Youanmi	Dromedary Bore Granodiorite, Thundelarra Supersuite	syenogranite gneiss	198213	2945	6	Wingate et al. (2015a)	
Yalgoo	Kynea Migmatite, Thundelarra Supersuite	granodiorite gneiss	155879	2950	-	Wingate et al. (2015c)	
Yalgoo	Kynea Migmatite, Thundelarra Supersuite	metatonalite	209689	2960	10	Lu et al. (2017a)	
DISTAL GNEISSES							
Southern Cross	unassigned	metasyenogranite	199022	2914	3	Lu et al. (2017b)	
Southern Cross	unassigned	metasyenogranite	205916	2921	9	Thebaud et al. (2013a)	
Southern Cross	unassigned	granodiorite gneiss	205912	2931	5	Thebaud et al. (2013b)	
Jerramungup	unassigned	metamonzogranite	224351	2940	6	Lu et al. (2019)	
Moora, Dookaling area	unassigned	granitic gneiss	99967082C	2940	5	Fletcher and McNaughton (2002)	xenocrystic component
Marymia	unassigned	granitic gneiss	216142	2980	18	Lu et al. (2017c)	
Southern Cross	unassigned	granodiorite gneiss	YQ38	2978	12	Qiu et al. (1999)	discordant analyses of inherited zircon cores
Byro	unassigned	orthogneiss	105002	2994	6	Nelson (1996)	
Maynard Hills	unassigned	quartzite	GSWA samples	c. 3000	-	Thern and Nelson (2016)	maximum depositional and crosscutting vein constraints
Toodyay	unassigned	quartzite	177904	3005	26	Wingate et al. (2008b)	maximum age of deposition
Moora, Coolangatta area	unassigned	granitic gneiss	99969093B	3007	3	Fletcher and McNaughton (2002)	
Calingiri	unassigned	monzogranitic gneiss	205930	3010	4	Wingate et al. (2018b)	
Marda	unassigned	granitic gneiss	121508	3014	17	Dalstra (1995)	reinterpreted as a xenocrystic population
Byro	unassigned	metasandstone	142986	3064	17	Nelson (2000)	maximum age of deposition
Gum Creek	unassigned	felsic volcaniclastic rock	93-998	2965	21	Wang et al. (1998)	xenocrystic component
EASTERN GOLDFIELDS SUPERTERRANE							
Merolia Domain	unassigned	quartzite	185979	2910	14	Wingate et al. (2011a)	maximum age of deposition
Norseman	Penneshaw Formation	rhyolite	104963	2930	4	Nelson (1995b)	
Yamarna	unassigned	tonalite	179448	2932	3	Wingate et al. (2011b)	
Duketon	unassigned	granodiorite	2001969122	2939	6	Dunphy et al. (2003)	
Merolia Domain	unassigned	metadacite	193363	2958	5	Wingate et al. (2010)	
Sir Samuel	unassigned	granodiorite	96969042	2959	3	Dunphy et al. (2003)	

To the south of the Gossan Hill Formation outcrop area, the Minjar Member truncates the underlying members, and it is itself truncated in part by unconformably overlying mafic volcanic rocks of the c. 2.79 Ga Polelle Group (Fig. 2). All these units are crosscut by felsic intrusive rocks of the Big Bell Suite at the southeastern extent of the Gossan Hill Formation. A 2.5 km-wide raft of Gossan Hill Formation, comprising the Scuddles and Golden Grove Members, forms an inclusion within a metagranite pluton of the Big Bell Suite, about 5 km north of the main Gossan Hill Formation outcrop area.

Metagranodiorite to metatonalite plutons assigned to the Gnows Nest Granodiorite of the Thundelarra Supersuite truncate the base of the succession in the east. These plutons form most of the eastern margin of the Gossan Hill Formation along a strike length of about 48 km and they are up to about 2.5 km wide. The plutons do not entirely crosscut the Scuddles Member and have not been observed to crosscut the Minjar Member. The Gnows Nest Granodiorite, which is locally schistose, replaces the Shadow Well Formation (Clifford 1992; Sharpe and Gemmel, 2001; Table 1) and quartz–feldspar schist is interpreted here to be a metagranitic rock rather than a metasedimentary rock, based on drillcore observations of porphyritic and equigranular plutonic textures, which are well preserved away from shear zones. Extensive dacitic dykes documented in drillcore logs within the Golden Grove and Gossan Valley Members have led to the hypothesis that these were subvolcanic to the Scuddles Member. These dykes do not crosscut the Gnows Nest Granodiorite. The Gnows Nest Granodiorite grades into subvolcanic dacitic rocks of the Scuddles Member at WAROX field location TJIGGR130058 (Zone 50, MGA 491513E 6828113N). In this area, there is an intimate relationship between granodiorite and dacite, in which decametre-scale apophyses of fine-grained granodiorite interfinger with dacite. The Gossan Hill Formation is also intruded by numerous and locally voluminous mafic–ultramafic sills and dykes, interpreted to belong to the c. 2790 Ma Warriedar Suite (Ivanic, 2019).

Mapping on the Badja and Thundelarra 1:100 000 map sheets (Zibra et al., 2016; Zibra et al., 2017) from 2012 to 2014 shows that the Mougooderra Formation unconformably overlies the Gossan Hill Formation (after Watkins and Hickman, 1990), and that the basalt-dominated succession previously referred to in part as the conformable, 'Thundelarra Group' (Clifford, 1992; Sharpe and Gemmel, 2001), was assigned to the Polelle Group. Our new interpretation of a double unconformity is shown in Figure 2 and is based on consideration of a non-structural truncation of the members of the Gossan Hill Formation to the southwest along a north-northwest trending region of non-exposure, which is weakly visible in aeromagnetic data. The Mougooderra Formation truncates both the Polelle Group and the Gossan Hill Formation about 1 km northwest of the Golden Grove mine site along a north-northwest-trending unconformity. North of this point the western margin of the Gossan Hill Formation is in sheared contact with younger greenstones and shows higher degrees of shearing close to the Mougooderra Shear Zone (Fig. 2, inset).

To the east of the Gossan Hill Formation and Gnows Nest Granodiorite lie deeply weathered but distinctly metagranitic rocks that are assigned to the Big Bell Suite based on the U–Pb zircon age of 2710 ± 7 Ma (Schiøtte and Campbell, 1996). This pluton is interpreted to truncate the older greenstone successions to the west and in places host large 5 km-scale rafts of greenstones such as the one in the northern part of the inset in Figure 2.

Methods

Geological mapping

Mapping was conducted during several field seasons between 2013 and 2018. Mapping within the Golden Grove mining leases was conducted in 2013, with the assistance and supervision of MMG Ltd staff. During mapping, field observations were recorded (see Fig. 5) and samples were collected for geochronology, geochemistry and petrography from outcrops and from drillhole intersections of the freshest and least deformed volcanic and plutonic rocks.

Whole-rock geochemistry

A total of 36 whole-rock compositions are reported here (Appendix 1). Samples were crushed in a steel plate jaw crusher and then pulverized to a fine powder. Thirty samples were pulverized in tungsten carbide ring mills, while the remaining six samples were pulverized in low-Cr steel ring mills. Due to several years of sample analyses in this sample set, the sample compositions were determined by three laboratories, including Intertek Genalysis Laboratory Services Pty Ltd (Genalysis; n = 32) and Australian Laboratory Services Pty Ltd (ALS; n = 1) in Perth and Geoscience Australia (GA; n = 3) in Canberra.

Major and minor element oxides were determined by wavelength dispersive x-ray fluorescence spectrometry (XRF) on fused disks prepared by fusing a 1:10 sample-flux mix (typically 0.7 g of sample powder with 7 g $LiBO_2$, LiB_4O_7 and $LiNO_3$ flux) at ≥1025ºC. Major and minor element oxides are reported on an anhydrous basis and all Fe is reported as Fe_2O_3 (i.e. Fe_2O_3T). Loss on ignition (LOI) was determined by thermogravimetric analysis.

Methods for trace-element determinations varied between laboratories. Genalysis determined concentrations of lithophile trace elements by mixing sample material with lithium borate flux in a platinum crucible and fusing at 1000 °C then dissolving the fusion product in HCl. The resulting solutions were then diluted before analysis by inductively coupled plasma mass spectrometry (ICP-MS; Cs, Rb, Ba, Sr, Th, U, Nb, Ta, Zr, Hf, Y, La, Ce, Pr, Nd, Sm, Eu, Gd, Tb, Dy, Ho, Er, Tm, Yb, Lu, Sn, W, V and Ga) or inductively coupled plasma optical emission spectrometry (ICP–OES; V, Sc, Cr). ALS used a similar fusion-based digestion method for lithophile trace elements but determined all analytes by ICP-MS. Genalysis determined concentrations of base metals by digesting sample material in a 4-acid mixture ($HClO_4$, HNO_3, HF and HCl) then diluting and analysing the solution by ICP-MS (Ag, As, Be, Bi, Cd, Co, Ge, In, Li, Mo, Pb, Sb) or by ICP–OES (Cu, Ni and Zn). ALS used a similar digestion method for base metals, but solutions were analysed by inductively coupled plasma atomic emission spectrometry (ICP–AES).

Figure 5. Field and hand specimen photographs of a range of lithologies from 3.0 – 2.9 Ga units of the Youanmi Terrane: a) rhyodacitic volcaniclastic rocks in drillcore from the Golden Grove Member, Golden Grove mine; b) the Gnows Nest Granodiorite in drillcore (GSWA 207683); c) cuprite nodule mantled by malachite, showing expansion cracks into altered dacite of the Scuddles Member, Gossan Hill open pit; d) flow-banded rhyolite cut by glassy grey dacite (left) from the middle Madoonga Formation, Mindoolah area; e) ball-and-pillow structures within rhyolite of the upper Madoonga Formation, northwestern Weld Range, indicating mafic–felsic magma mingling; f) recrystallized amygdaloidal andesite of the Annabelle Volcanics, 4 km north of Ravensthorpe; g) coarse hornblende tonalite, Manyutup Tonalite, 12 km southwest of Ravensthorpe; h) polyphase deformation within migmatitic metatonalite of the Kynea Migmatite, core of the Yalgoo Dome; i) multiple intrusions and fabrics in TTG gneiss, 45 km south of Twin Peaks; j) stretched pebbles in the Mougooderra Formation, Warriedar Hill

GA determined concentrations for trace elements Cr, Cu, F, Ni, V, Zn, and Zr by XRF on a 'pressed pellet', using methods like those of Norrish and Chappell (1977), whereas they determined the remaining trace-element concentrations by ICP-MS using methods similar to those of Eggins et al. (1997), but on solutions obtained by dissolution of fused glass disks (Pyke, 2000). Concentrations of precious metals (Au, Pd and Pt) were determined by Genalysis and ALS by Pb collection fire assay and ICP-MS.

Data quality at the three laboratories are broadly comparable, with total uncertainties for major elements ≤1.5 %, minor elements <2.5 % (at concentrations >0.1 wt. %) and those for trace elements are ≤10 % (Lu ± 20 %).

U–Pb geochronology

Samples for Sensitive High-Resolution Ion Microprobe (SHRIMP) U–Pb zircon geochronology were collected from five drillcores (GSWA 203701, 203702, 203703, 203704 and 207683) and from eight surface outcrops (Table 2). Geochronological data are reported in Appendix 2. Zircons were analysed using SHRIMP II ion microprobes at the John de Laeter Centre at Curtin University, using procedures detailed in Wingate and Lu (2017). The zircons were cast, together with zircon reference standards, in epoxy discs, which were polished to expose the interiors of the crystals. The zircons were examined and documented in transmitted and reflected light, and in cathodoluminescence (CL) images (Fig. 6). Absolute U and Th concentrations and $^{238}U/^{206}Pb$ ratios were determined relative to zircon standards, analyses of which were interspersed with those of unknown zircon grains, as described in the individual Geochronology Records cited below. The OGC1 standard (3465.4 ± 0.6 Ma; Stern et al., 2009) was used to monitor $^{207}Pb^*/^{206}Pb^*$ reproducibility and accuracy (Pb* = radiogenic Pb). Data were reduced and analysed using SQUID and Isoplot (Ludwig, 2001, 2003), using decay constants recommended by Steiger and Jäger (1977). Correction for initial or common Pb was made using measured $^{204}Pb/^{206}Pb$ and contemporaneous common-Pb isotope compositions determined according to the model of Stacey and Kramers (1975) and plotted on concordia diagrams (Fig. 7). Mean ages are reported with 95% confidence intervals.

Lutetium–hafnium isotope analysis

Twenty samples were analysed for lutetium–hafnium isotopes (Appendix 3). Zircons from these samples were previously dated by GSWA. Lutetium–hafnium isotope analyses were conducted using a New Wave/Merchantek LUV213 laser-ablation microprobe attached to a Nu Plasma multicollector inductively coupled plasma mass spectrometer (LA-MC-ICP-MS). The analyses used a beam diameter of about 55 µm and repetition rate of 5 Hz, which produced typical ablation pits 40–60 µm deep. The ablated material was transported to the ICP-MS torch by helium carrier gas.

Interference of ^{176}Lu on ^{176}Hf was corrected by measurement of interference-free ^{175}Lu and using the recommended $^{176}Lu/^{175}Lu = 0.02669$ (DeBievre and Taylor, 1993). Interference of ^{176}Yb on ^{176}Hf was corrected by measuring the interference-free ^{172}Yb isotope and using the $^{176}Yb/^{172}Yb$ ratio to obtain the interference-free $^{176}Yb/^{177}Hf$ ratio. The appropriate value of $^{176}Yb/^{172}Yb$ was determined by spiking the JMC475 hafnium standard solution with Yb and determining the value of $^{176}Yb/^{172}Yb$ (0.58669) required to yield the $^{176}Hf/^{177}Hf$ value for the unspiked solution.

Two zircon standards, including Mud Tank and Temora-2, were analysed to evaluate the accuracy of the laser-ablation results. Thirty-nine analyses of Mud Tank zircon throughout the session yielded a mean $^{176}Hf/^{177}Hf$ value of 0.282510 ± 0.000016 (std.dev), consistent with the recommended value of 0.282507 ± 0.000006 (Woodhead and Hergt, 2005). Analytical results obtained from Temora-2 (mean $^{176}Hf/^{177}Hf = 0.282670 \pm 0.000019$, n = 29) agree with the accepted solution value (0.282686 ± 0.000008, Woodhead and Hergt, 2005).

Initial $^{176}Hf/^{177}Hf$ and εHf values of all zircons were calculated using the ^{176}Lu decay constant of Söderlund et al. (2004) and the CHUR (Chondritic Uniform Reservoir) value of Bouvier et al. (2008). For each analysis, a two-stage depleted mantle model age (T_{DM}^2) is calculated, which assumes that the parental magma of the zircon was produced from a volume of average continental crust ($^{176}Lu/^{177}Hf$ ratio of 0.015) extracted from depleted mantle (Griffin et al., 2000, 2004). T_{DM}^2 estimates the average age of the crustal source of the igneous rocks (Griffin et al., 2004). All analyses are of zircons with measured U–Pb compositions that are <10% discordant.

Results

Geological mapping and sampling

Figure 2 shows the simplified interpreted geology in the Yalgoo area. Map data at 1:500 000 and 1:100 000 has been compiled in digital form and is publicly available within the Youanmi GIS 2020 data package (GSWA, 2020). Explanatory notes are available on GeoVIEW (dmirs.wa.gov.au/geoview) and field observations are also available on GeoVIEW as well as in the WAROX 2021 data package (GSWA, 2021). Revised stratigraphic nomenclature is registered in Geoscience Australia's Australian Stratigraphic Units Database.

The results of stratigraphic observations are summarized in Figure 4a and Table 3, which highlight that the successions share a felsic volcanic component and are typically overlain by a siliciclastic and/or BIF package. These observations also identify more subvolcanic felsic to intermediate plutons, which have now been observed in half of the successions (Fig. 4). Figure 5 shows examples of notable meso-scale observations from representative units in drillcore, outcrops and hand specimens and augments previous work in these localities (e.g. Witt, 1998; Guilliamse, 2014; Clifford, 1992; Watkins and Hickman, 1990; Foley, 1997). The formations contain variable thicknesses of mafic–intermediate volcanic rocks, which are either above, below or interlayered with felsic volcanic rocks. The formations also contain variable amounts of volcaniclastic rock and the thicknesses of banded iron-formation involved are highly variable.

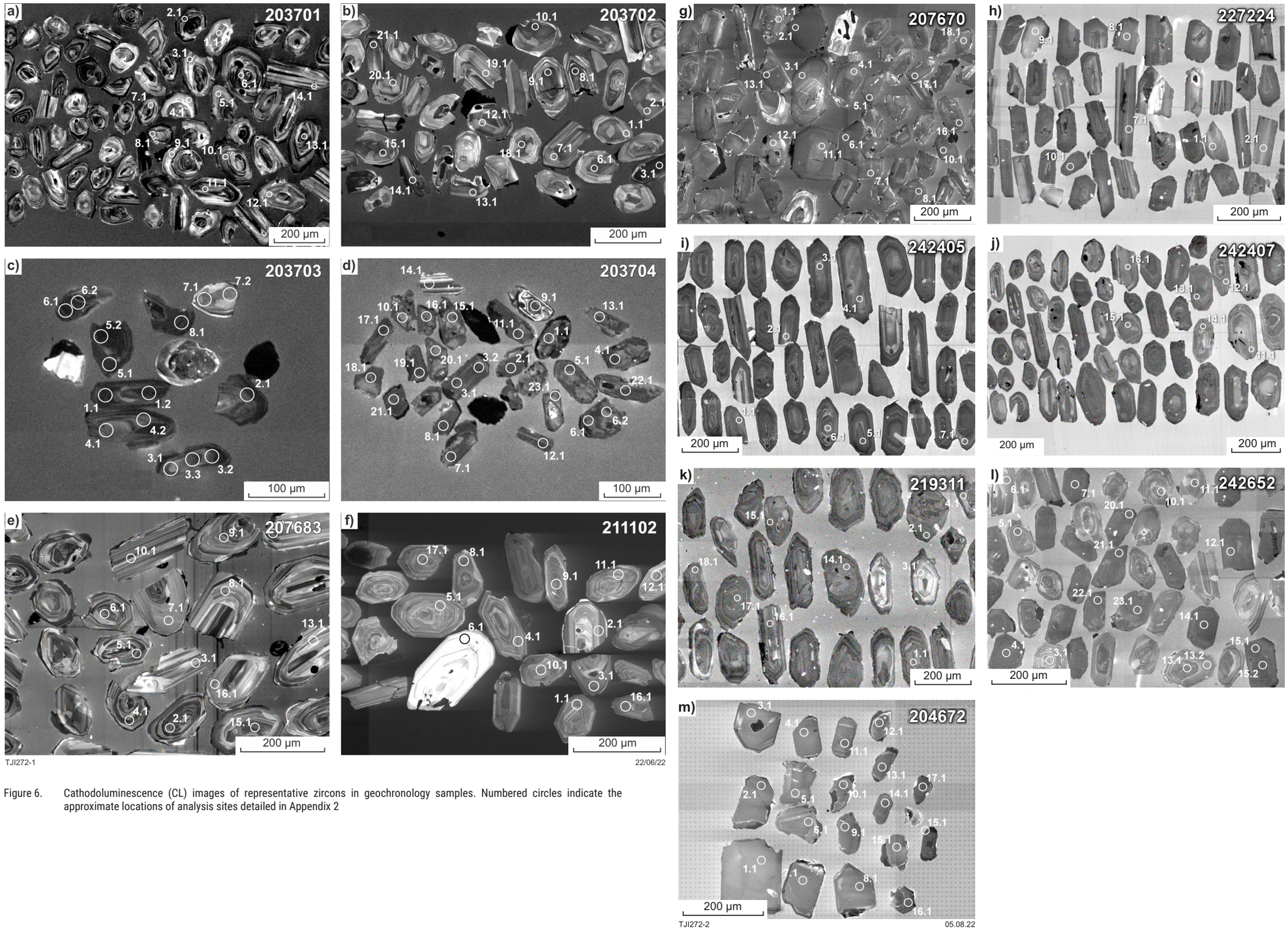

Figure 6. Cathodoluminescence (CL) images of representative zircons in geochronology samples. Numbered circles indicate the approximate locations of analysis sites detailed in Appendix 2

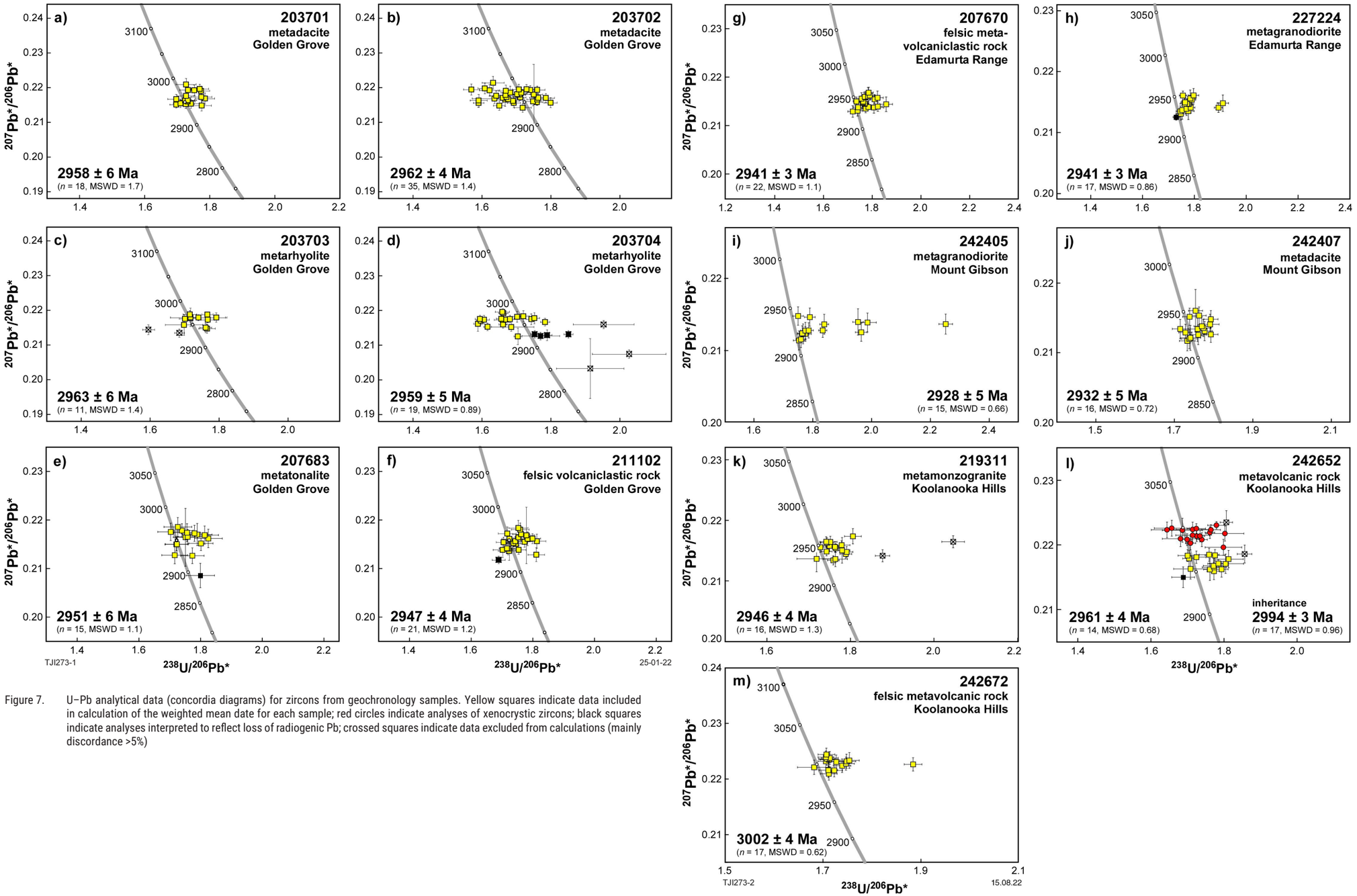

Figure 7. U–Pb analytical data (concordia diagrams) for zircons from geochronology samples. Yellow squares indicate data included in calculation of the weighted mean date for each sample; red circles indicate analyses of xenocrystic zircons; black squares indicate analyses interpreted to reflect loss of radiogenic Pb; crossed squares indicate data excluded from calculations (mainly discordance >5%)

Table 3. Characteristics of selected 3.01 – 2.92 Ga rock units of the Youanmi Terrane

Stratigraphic name	*Location*	*Mineral deposits (minor in brackets)*	*Lithology (metamorphosed)*	*Associated lithologies (minor)*	*No. of samples dated*	*Isotopic age (Ma)*	*Approx. stratigraphic thickness (km)*	*Approx. strike length / pluton diameter (km)*
unassigned	Tallering	-	tonalite	-	1	2918		25
Honman Formation	Lake Johnston	Ni–Co	rhyolite–dacite	basalt, komatiite	6	2920	<1	15
Mount Gibson Formation	Mount Gibson	Au (Pb–Zn–Ag) Fe-BIF	rhyolite–dacite	basalt	3	2931	1–2	15
Great Northern granodiorite	Mount Gibson	-	granodiorite	-	2	2935		15
unassigned	Tallering	(Cu–Pb–Zn–Ag–Au) Fe-BIF	rhyolite–dacite	basalt	1	2935	2–4	50
unassigned	Edamurta Range	Cu–Pb–Zn	rhyolite–dacite	basalt	1	2940	2	10
Gnows Nest Granodiorite	Golden Grove	(Au)	granodiorite	-	1	2951		50
Annabelle Volcanics (II)	Ravensthorpe	Cu–Au (Ag) (Mn)	dacite–andesite	(basaltic andesite)	2	2958	2–3	50
unassigned	Koolanooka Hills	(Au) Fe-BIF	rhyolite–dacite	basalt, high-Mg basalt	1	2961	2–4	15
Gossan Valley Member	Golden Grove	Cu–Au–Zn–Ag–Pb	rhyolite–dacite	(basalt)	7	2961	3	50
Annabelle Volcanics (I)	Ravensthorpe	Cu–Au (Ag) (Mn)	dacite–andesite	(basaltic andesite)	2	2989	2–3	50
Manyutup Tonalite	Ravensthorpe	(Cu–Au)	tonalite	(diorite–gabbro)	2	2984		20
Madoonga Formation	Weld Range	(Au–Ag–Zn–Pb–Cu) Fe-BIF	rhyolite–dacite	basalt, high-Mg basalt	4	2975	4–6	35
Mindoolah Tonalite	Weld Range	(Au)	tonalite	-	1	2998		2
unassigned	Koolanooka Hills	(Au) Fe-BIF	rhyolite–dacite	basalt, high-Mg basalt	2	3002	2–4	15
unassigned	Twin Peaks	(Cu–Pb–Zn–Ag–Au) Fe-BIF	rhyolite–dacite	(basaltic andesite)	1	3005	2–4	25
unnamed	Twin Peaks	-	granitic rocks	-	1	3003		20
unassigned	Wongan Hills	Cu–Pb–Zn–Ag–Au	rhyolite–dacite	basalt	1	3010	3	25
unnamed	Wongan Hills	-	granitic rocks	-	3	3010		20

Whole-rock geochemistry

Whole-rock geochemistry is described below for 36 igneous samples collected from outcrops and drillcores, which are interpreted to belong to 3.0 – 2.9 Ga lithostratigraphic associations in the Yalgoo–Golden Grove and Weld Range areas. These samples are mostly from the Gossan Hill Formation (n = 20), with fewer samples from the Madoonga Formation (n = 4) and an unnamed succession at Edamurta (n = 1). The compositions of 11 plutonic or gneissic rocks interpreted to belong to the 3.0 – 2.9 Ga Thundelarra Supersuite are also shown for comparison, predominantly from the Kynea Migmatite (n = 10) in the Yalgoo Dome, and one sample from the Gnows Nest Granodiorite in the Golden Grove area. These data are available in GSWA's state geochemical database (WACHEM; **dmirs.wa.gov.au/geochem**) and are included in Appendix 1.

The dataset has been filtered to exclude samples with strongly altered compositions. Samples containing ≥75 wt% SiO_2 were excluded from the dataset if Na_2O < 0.5 wt% or Al_2O_3 >20 wt%. Samples containing ≥75 wt% SiO_2 are almost certainly silicified, although their exclusion would remove nearly all the Madoonga Formation samples, which appear to retain reliable incompatible trace-element ratios. One sample from the Madoonga Formation was excluded because its REE concentrations are significantly elevated compared to other samples in the unit and are enriched compared to similarly incompatible high field strength elements (i.e. it showed a strongly negative Zr–Hf anomaly), suggesting enrichment via secondary alteration. The compositional filtering process significantly reduced the number of viable 3.0 – 2.9 Ga volcanic samples and highlights that most samples reported to date are moderately to strongly altered, which appears to have had a stronger effect on the major elements than on the incompatible trace elements.

Major and trace elements

Figure 8 shows the total alkalis vs silica classification for plutonic and volcanic rocks analysed in this study. After alteration filters were applied to the dataset, the remaining data range from 64.4 to 78.7 wt% SiO_2. Plutonic rocks classify as granodiorite to granite (Fig. 8a; after Middlemost, 1994) and volcanic rocks mostly classify as dacite to rhyolite (Fig. 8a; after Le Maitre et al., 1989) on total alkali vs silica schemes. Figure 9 shows major and minor elements and selected trace elements plotted against SiO_2. Volcanic rocks show negative trends between SiO_2 and CaO, MgO, TiO_2, Al_2O_3, P_2O_5, Cr and Ni (Fig. 9a–l).

Gossan Hill Formation and Gnows Nest Granodiorite

Nearly all Gossan Hill Formation samples have consistently high large ion lithophile elements (LILEs; Cs, Rb, Ba, K) and Th, with negative Nb–Ta anomalies (relative to mantle-normalized Th and La) and positive Zr–Hf anomalies (relative to Sm and Nd). Three samples have very low K_2O and lower Cs, Rb, Ba compared to the other Gossan Hill Formation samples, which likely reflects depletion of these relatively mobile elements via secondary alteration. The single Gnows Nest Granodiorite sample plots together with the Gossan Hill Formation on all compositional diagrams.

On primitive mantle-normalized trace-element diagrams (Fig. 10), all Gossan Hill Formation and Gnows Nest Granodiorite samples have similarly enriched light to middle rare earth element (LREE–MREE) patterns but can be separated into three chemical groups based on their HREE characteristics. The first group, of seven samples (Fig. 10b,d) including the Gnows Nest Granodiorite sample (Fig. 10a,c), has dacitic bulk compositions and spoon-shaped REE patterns, with $[Gd/Yb]_{PM}$ of 1.7 – 2.3 and 0.9 – 1.4 ppm Yb. The second group (Fig. 10b,d), of two samples, has rhyolitic bulk compositions, $[Gd/Yb]_{PM}$ of 2.2 – 3.4 and contains notably lower HREEs (approximately 0.4 ppm Yb) – compositionally similar to samples from the Kynea Migmatite (described below). The HREE-depleted patterns of the first and second groups (yellow and pink symbols, respectively in Fig. 10b,d) could be attributed to residual garnet and/or amphibole in their sources, or magmatic fractionation of hornblende, or both. The third group, of nine samples (Fig. 10b,d), also indicates rhyolitic bulk compositions, but much lower $[Gd/Yb]_{PM}$ of 0.7 – 0.9 and notably higher HREEs (4.7 – 6.3 ppm Yb). Primitive mantle-normalized REE patterns of the third group (red symbols in Fig. 10) show overall very high REE concentrations, LREE>MREE and MREE<HREE and strong negative Eu anomalies, i.e. birdwing-shaped (Fig. 10d). The strong negative Eu anomalies (Eu/Eu* = 0.5 – 0.6) reflect significant fractionation of plagioclase. Rhyolites and granitic rocks with similarly shaped REE patterns have been attributed elsewhere to high degrees of magmatic fractionation (consistent with strong Eu anomalies and very high SiO_2 concentrations in this study) or precipitation of HREE-bearing minerals from hydrothermal fluids (e.g. Elliott, 2018).

Madoonga Formation

All Madoonga Formation samples in this study have very high SiO_2 (75.7 – 78.7 wt%), i.e. they are clearly intensely fractionated but also almost certainly silicified. Rare earth element patterns are again birdwing-shaped (Fig. 10b,d), but mostly at lower HREE concentrations compared to samples with similarly shaped REE patterns in the Gossan Hill Formation.

Edamurta succession

The single volcanic rock from the Edamurta succession collected for geochronology and geochemistry has a dacitic composition (Fig. 8b), with moderate to low Mg-number (42), Ni (26 ppm) and Cr (45 ppm). It contains lower Al_2O_3 than the Gossan Hill and Madoonga Formations and negligible K_2O (<0.1 wt%), although with so few samples it is unclear whether this reflects an altered composition. The trace-element pattern for this sample is LREE-enriched (Fig. 10b,d), with a slightly positive Eu anomaly that could reflect excess plagioclase or alteration. REE concentrations are generally high compared to other samples in this study, comparable to the highly fractionated end-member samples from the Gossan Hill and Madoonga Formations.

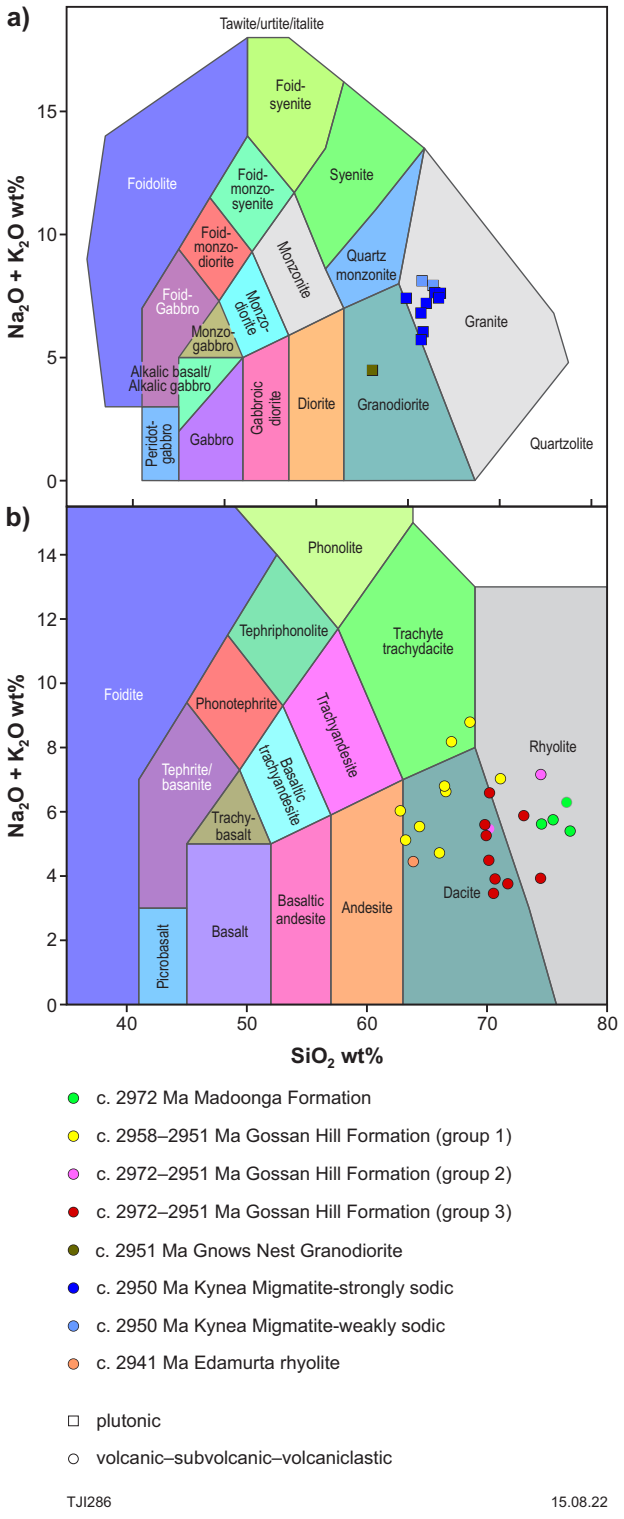

Figure 8. Total alkalis vs silica plots in wt% for a) plutonic rocks, b) volcanic rocks

Kynea Migmatite

Samples of the Kynea Migmatite are typically gneissic, tonalitic and compositionally layered. They define more discrete trends on plots of major elements against silica (Fig. 9a–l), suggesting these rocks were not strongly affected by hydrothermal alteration. Kynea Migmatite samples contain high SiO_2 (70–74 wt%), are strongly sodic (K_2O/Na_2O mostly 0.3 – 0.6 with two samples slightly higher at 0.8 and 0.9), have high Al_2O_3 (14.7 – 16.4 wt%), Sr (230–720 ppm) and Sr/Y (48–222 ppm) and relatively low Mg-numbers (<40), Ni (≤ 10 ppm) and Cr (≤ 30 ppm). Trace-element patterns are strongly LREE enriched, with depleted HREEs (Fig. 10a). These are interpreted as typical TTG compositions and are attributed to residual garnet in their lower mafic crustal sources.

U–Pb geochronology

Thirteen geochronology samples and analytical results are described in this section and summarized in Table 2 and Figure 11. The samples include five volcanic rocks and one plutonic rock from the Golden Grove mining area, and five volcanic rocks and two plutonic rocks from the Edamurta, Koolanooka and Mount Gibson areas of the wider Yalgoo–Singleton greenstone belt. Cathodoluminescence (CL) images and concordia diagrams are provided in Figures 6 and 7, respectively. More detailed information for each sample is available in Geochronology Records cited in Table 2, and U–Pb analytical data are provided in Appendix 2.

GSWA 203701: metadacite, Golden Grove

This Scuddles Member metadacite was sampled from core drilled about 11 km north-northwest of the Golden Grove mine area. The sample of consists of about 70% quartzofeldspathic groundmass, 20–25% plagioclase phenocrysts, 4–5% quartz phenocrysts, 3% ferromagnesian phenocrysts, and trace opaque minerals. Plagioclase (andesine, An_{38}) phenocrysts are euhedral to subhedral and tabular and up to 2 mm long. Quartz phenocrysts are up to 2 mm in size and display delicate embayment and pseudo-hexagonal crystal shapes. Some quartz is weakly undulose. The rock exhibits minor alteration to fine-grained chlorite and less abundant white mica, epidote, and carbonate.

Zircons isolated from this sample are colourless to pale brown, up to 300 µm long, subhedral to euhedral, and equant to elongate, with aspect ratios up to 4:1. In CL images, concentric zoning is ubiquitous (Fig. 6a). Eighteen analyses of 18 zircons (Appendix 2) are concordant to slightly discordant and form a single group (Fig. 7a), with a weighted mean $^{207}Pb^*/^{206}Pb^*$ date of 2958 ± 6 Ma (MSWD = 1.7), interpreted as the igneous crystallization age of the dacite.

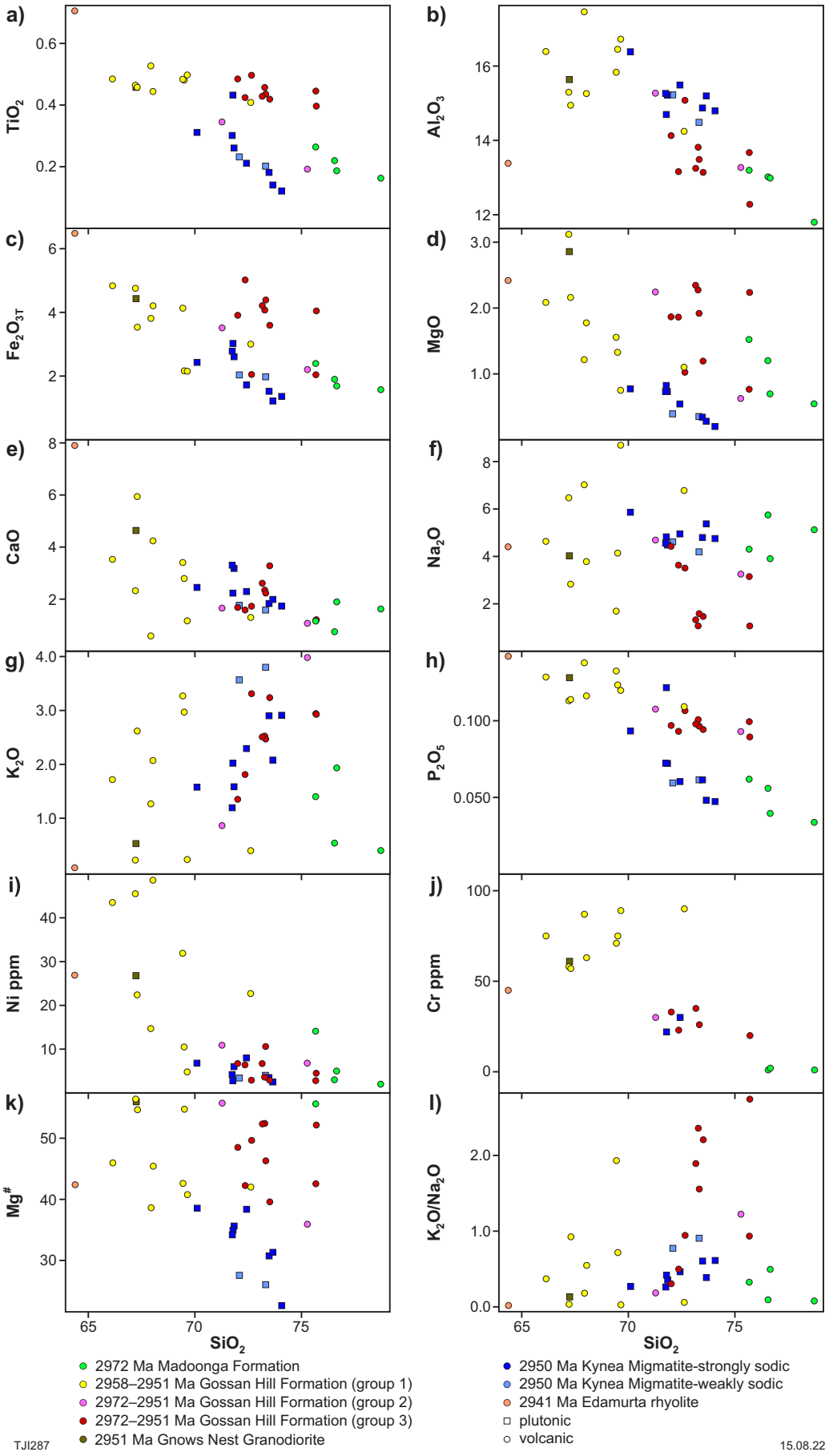

Figure 9. Harker variation diagrams in wt% for the Gossan Hill Formation, Madoonga Formation, Gnows Nest Granodiorite, Kynea Migmatite and the Edamurta succession: a) SiO_2 vs TiO_2; b) SiO_2 vs Al_2O_3; c) SiO_2 vs $Fe_2O_3^T$; d) SiO_2 vs MgO; e) SiO_2 vs CaO; f) SiO_2 vs Na_2O; g) SiO_2 vs K_2O; h) SiO_2 vs P_2O_5; i) SiO_2 vs Ni; j) SiO_2 vs Cr; k) SiO_2 vs Mg#; l) SiO_2 vs (K_2O/ Na_2O)

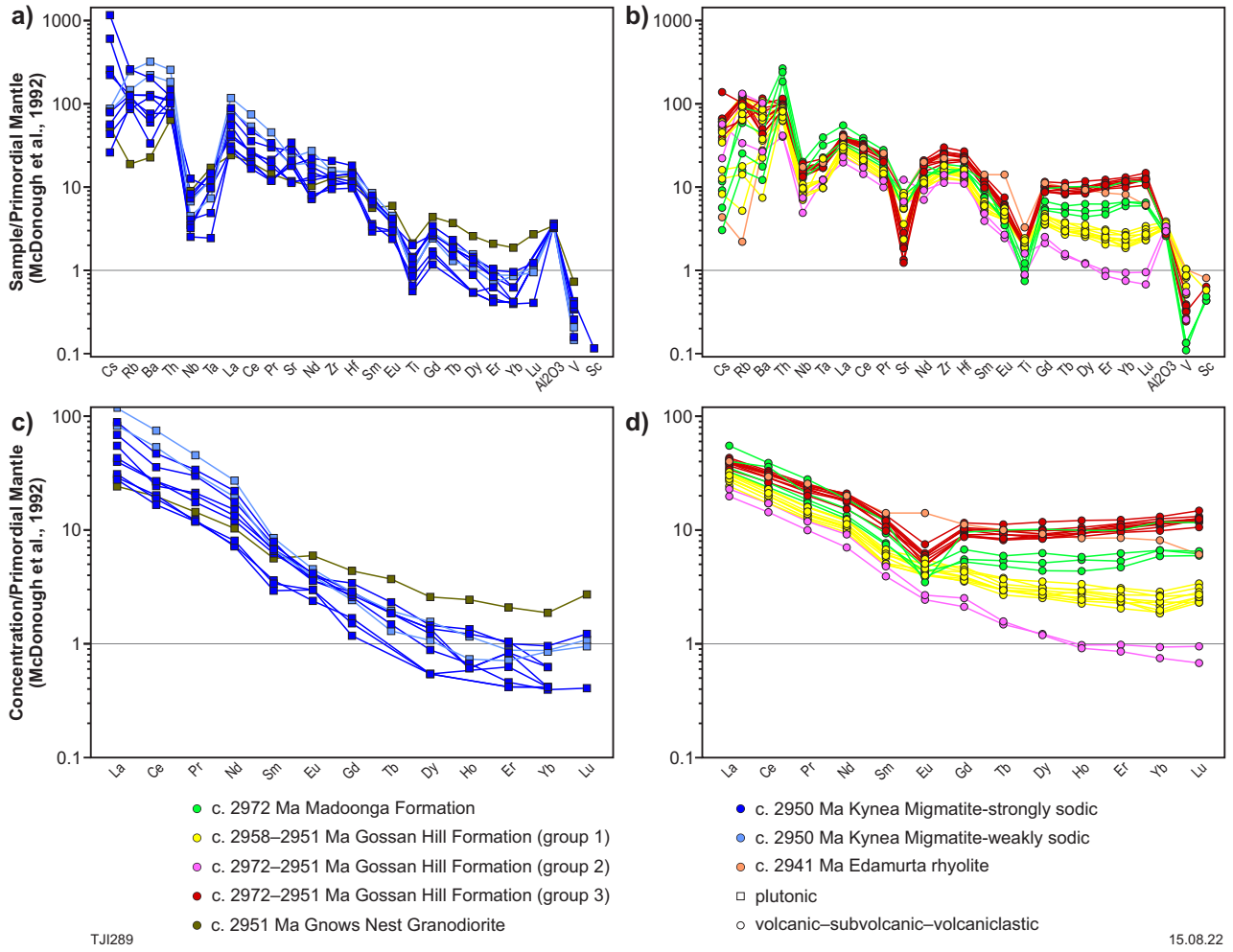

Figure 10. Trace-element variation diagrams (spidergrams) for: a) plutonic rocks; b) volcanic and subvolcanic rocks; c) plutonic rocks, REE; d) volcanic rocks, REE. Normalization to primitive mantle is after McDonough and Sun (1995)

GSWA 203702: metadacite, Golden Grove

This drillcore sample of Scuddles Member from the Golden Grove mine is a porphyritic metadacite, consisting of about 65–70% aphanitic matrix, 20% plagioclase, 10% actinolite, and accessory chlorite, epidote, and opaque oxide minerals. The matrix is crypto- to microcrystalline (grain size up to 0.05 mm), and composed mainly of sericite, quartz and feldspar. Plagioclase (andesine, $An_{30–34}$) forms subhedral to euhedral lath-shaped, partially resorbed phenocrysts, up to 0.8 mm long, clouded by saussurite and rimmed by albite. Actinolite occurs as sheaves of acicular crystals up to 0.1 mm long.

Zircons from the sample are colourless, subhedral to euhedral, up to 250 µm long, and equant to elongate, with aspect ratios up to 5:1. In CL images, concentric zoning is ubiquitous, and many crystals exhibit sector zoning (Fig. 6b). Thirty-five analyses of 35 zircons are concordant to slightly discordant (up to 7%) and form a single group (Fig. 7b), with a weighted mean $^{207}Pb^*/^{206}Pb^*$ date of 2962 ± 4 Ma (MSWD = 1.4), interpreted as the igneous crystallization age.

GSWA 203703: metarhyolite, Golden Grove

The drillcore sample of metarhyolite from the Golden Grove Member at the Golden Grove mine consists of a strongly foliated assemblage of micro- to cryptocrystalline quartz (mostly <0.02 mm) intergrown with aligned sericite (mostly <0.05 mm). Minor to trace components include possible sillimanite, chloritoid, clinozoisite, epidote, and iron–titanium oxide minerals. Clouded pseudomorphs and irregular aggregates may represent unidentified deformed and recrystallized components.

Only 10 zircons were isolated from this sample. They are colourless, anhedral to subhedral, up to 300 µm long, and equant to slightly elongate, with aspect ratios up to 4:1. In CL images, all crystals exhibit concentric zoning, and one zircon exhibits sector zoning (Fig. 6c). Fifteen analyses were obtained from eight zircons (Appendix 2). Two analyses that yield significantly younger dates of 2930–2926 Ma, and two discordant analyses are excluded. Eleven analyses of seven zircons are concordant to slightly discordant and form a single group (Fig. 7c), with a weighted mean $^{207}Pb^*/^{206}Pb^*$ date of 2963 ± 6 Ma (MSWD = 1.4), interpreted as the igneous crystallization age of the rhyolite.

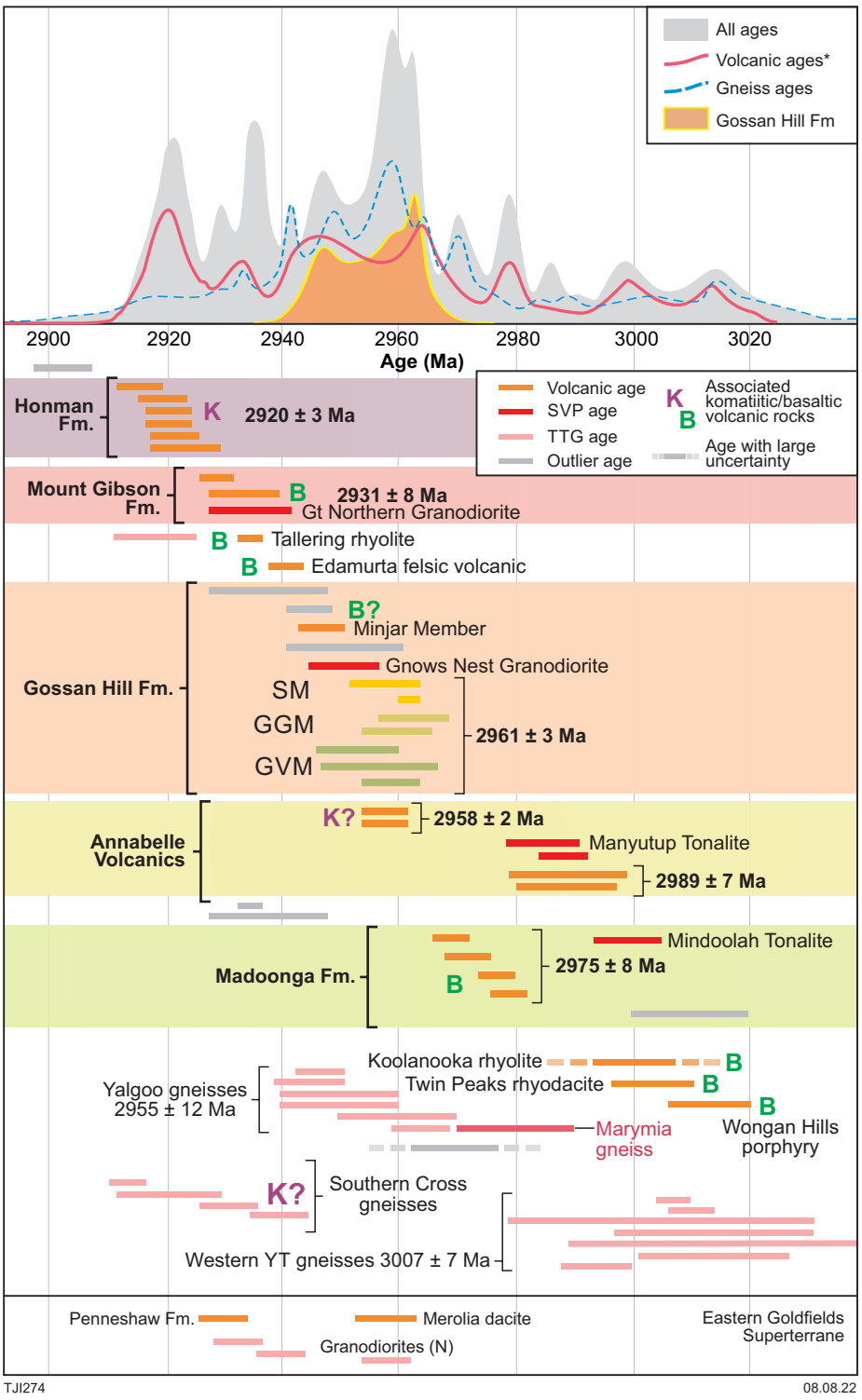

Figure 11. Summary of magmatic crystallization ages for selected 3.01 – 2.90 Ga rock units in the Youanmi Terrane. Horizontal bars indicate 95% confidence intervals). SVP = subvolcanic pluton, SM = Scuddles Member, GGM = Golden Grove Member, GVM = Gossan Valley Member, YT = Youanmi Terrane. Geochronology from sources in Table 2. *Volcanic age spectra do not include Gossan Valley Formation samples

GSWA 203704: metarhyolite, Golden Grove

This drillcore sample of the Gossan Valley Member at the Golden Grove mine is a metarhyolite or metarhyodacite and consists mainly (85–90%) of a strongly foliated matrix of micro- to cryptocrystalline (mostly <0.01 mm) quartz and sericite, 10% quartz phenocrysts, minor sericite pseudomorphs, and accessory epidote, clinozoisite, and iron–titanium oxide minerals. Quartz phenocrysts are up to 1 mm across, appear corroded, and are partially recrystallized. Sericite pseudomorphs, up to 1 mm across, may be after feldspar.

Only 25 zircons were isolated from this sample, and they are mainly colourless, subhedral to euhedral, up to 300 µm long, and slightly elongate, with aspect ratios up to 4:1. Concentric zoning is indistinct but ubiquitous in CL images (Fig. 6d). Nineteen analyses of 18 zircons are concordant to slightly discordant (Fig. 7d) and yield a weighted mean $^{207}Pb^*/^{206}Pb^*$ date of 2959 ± 5 Ma (MSWD = 0.89). Four analyses that yield significantly younger dates of 2930–2926 Ma, and three imprecise discordant analyses acquired during a period of instrument instability, are excluded (Appendix 2). The mean date of 2959 ± 5 Ma for 19 accepted analyses is interpreted as the igneous crystallization age of the rhyolite.

GSWA 207683: metatonalite, Golden Grove

This sample of Gnows Nest Granodiorite was drilled about 16 km northwest of the Golden Grove mine area. The sample is a weakly deformed, medium-grained metatonalite, consisting of about 60% plagioclase, 25% quartz, 5% biotite, 5% chlorite, 3–5% epidote, 1–2% opaque minerals, and accessory apatite and zircon. Plagioclase is finely sericitized and forms non-aligned aggregates of mainly subhedral equant to tabular grains. Quartz forms irregular, anhedral, interstitial grains that locally entirely enclose plagioclase. Quartz is strained to subgrained and includes minor finely recrystallized aggregates. Biotite ± chlorite crystals are up to 0.7 mm long, and typically form aggregates up to 3 mm diameter, with epidote-replaced grains and opaque minerals. The epidote-replaced grains are up to 1 mm in size, with regular, elongate outlines, and may be pseudomorphs after pyroxene or amphibole.

Zircons in this sample are colourless, subhedral to euhedral, up to 300 µm long, and equant to elongate, with aspect ratios up to 4:1. In CL images, all zircons exhibit concentric zoning (Fig. 6e). Sixteen analyses of 16 zircons are concordant to slightly discordant (Fig. 7e), and 15 analyses yield a weighted mean $^{207}Pb^*/^{206}Pb^*$ date of 2951 ± 6 Ma (MSWD = 1.1), interpreted as the igneous crystallization age. The single excluded analysis (Appendix 2) indicates a significantly younger date of 2895 ± 20 Ma (1σ).

GSWA 211102: felsic volcaniclastic rock, Golden Grove

This felsic volcaniclastic rock was sampled in outcrop about 7 km southeast of the Golden Grove mine area. The sample consists of about 80–85% microcrystalline, probable quartzofeldspathic matrix, 12–15% feldspar, 2–3% cherty grains, 1–2% quartz, 1% secondary iron oxide minerals, and accessory black opaque minerals, apatite, zircon, and secondary epidote and chlorite. The matrix includes a few slightly more coarsely crystalline fragments up to 0.1 mm long with rod-like to arcuate shapes that may have originally been non-welded relict glass shards. The possibility of non-welded shards supports a volcanic source, likely to represent contemporaneous volcanic activity rather than material eroded from older deposits. The rock is not deformed or metamorphosed beyond lower greenschist facies.

Zircons from this sample are colourless, subhedral to euhedral, up to 250 µm long, and equant to elongate, with aspect ratios up to 3:1, and exhibit concentric zoning (Fig. 6f). Twenty-four analyses of 24 zircons are concordant to strongly discordant (Fig. 7f). Excluding three analyses that yield significantly younger dates (Appendix 2), 21 analyses yield a weighted mean $^{207}Pb^*/^{206}Pb^*$ date of 2947 ± 4 Ma (MSWD = 1.2), interpreted as the igneous crystallization age.

GSWA 207670: felsic metavolcaniclastic rock, Edamurta Range

Collected from outcrop in the Edamurta greenstone belt, on the northwestern margin of the Yalgoo Dome, the sample is a strongly deformed, altered, felsic metavolcaniclastic rock. It consists of microcrystalline matrix containing about 15% feldspar and quartz phenocrysts, secondary epidote and actinolite, and minor lithic clasts, titanite, chlorite, and biotite. The matrix has a cherty appearance and contains extensive anastomosing and discontinuous folia and patches of fine alteration minerals, mainly epidote and actinolite. The rock has been strongly deformed at upper greenschist facies conditions (indicated by actinolite and trace biotite), resulting in a wavy tectonic foliation.

Zircons from this sample are colourless to pale purple, and mainly subhedral to euhedral. The crystals are up to 200 µm long, and equant to slightly elongate, with aspect ratios up to 4:1. In CL images, all zircons exhibit concentric zoning (Fig. 6g). Twenty-two analyses of 22 zircons are concordant to moderately discordant (Fig. 7g) and yield a weighted mean $^{207}Pb^*/^{206}Pb^*$ date of 2941 ± 3 Ma (MSWD = 1.1), interpreted as the igneous crystallization age of the dominant zircon-bearing volcanic component.

GSWA 227224: metagranodiorite, Edamurta Range

This metagranodiorite sample was collected from an outcrop in the Edamurta greenstone belt, on the northwestern margin of the Yalgoo Dome. The sample consists of about 50% plagioclase, 30% quartz, 10–12% K-feldspar, 7–8% biotite, <1% magnetite, and trace tourmaline, apatite and zircon. The granodiorite lacks a tectonic foliation but displays evidence of deformation and minor recrystallization at relatively low-grade metamorphic conditions.

Zircons from this sample are colourless to dark brown and mainly subhedral to euhedral. The crystals are up to 300 µm long, and elongate, with aspect ratios up to 9:1. In cathodoluminescence (CL) images, concentric zoning is ubiquitous, some crystals are dominated by high-U metamict zones, and a few crystals appear to contain older cores (Fig. 6h). Eighteen analyses of 18 zircons are concordant to moderately discordant (Fig. 7h), and 17 analyses yield a weighted mean $^{207}Pb^*/^{206}Pb^*$ date of 2941 ± 3 Ma

(MSWD = 0.86), interpreted as the igneous crystallization age. The single excluded analysis is of a high-U zircon and interpreted to reflect loss of radiogenic Pb.

GSWA 242405: metagranodiorite, Mount Gibson

This metagranodiorite of the Thundelarra Supersuite was sampled from outcrop west of the Mount Gibson mining area. The sample is medium-grained, consisting of about 35% plagioclase, 30% quartz, 20–25% K-feldspar, 7–8% biotite, 3% myrmekite, and trace magnetite, hematite, muscovite, apatite and zircon. The rock was probably originally equigranular, but is partially recrystallized, forming fine-grained patches of polygonal or anhedral grains. The sample lacks a foliation, although microcline twinning and undulose extinction are evidence of deformation and grain boundary adjustment. The recrystallized patches of fine-grained feldspar and quartz and development of myrmekite suggest metamorphism at relatively high-temperature amphibolite conditions.

Zircons isolated from this sample are colourless to dark brown or opaque, and subhedral to euhedral. The crystals are up to 350 µm long, and elongate, with aspect ratios up to 7:1. In CL images, concentric zoning is ubiquitous, and many crystals are dominated by high-U, metamict zones (Fig. 6i). Sixteen analyses of 16 zircons are concordant to strongly discordant (Fig. 7i). Excluding one highly discordant analysis, 15 analyses yield a weighted mean $^{207}Pb^*/^{206}Pb^*$ date of 2928 ± 5 Ma (MSWD = 0.66), interpreted as the igneous crystallization age.

GSWA 242407: metadacite, Mount Gibson

This drillcore sample came from Ninghan Station west of the Great Northern Highway. The sample is weakly laminated and consists of about 98–99% quartzofeldspathic groundmass, 1% quartz phenocrysts, <1% plagioclase phenocrysts, and minor apatite and zircon. The sample is mostly recrystallized to a microcrystalline aggregate of interlocking, polygonal grains. A weak, slightly wavy lamination is defined by discontinuous concentrations of biotite.

Zircons from this sample are pale brown to dark brown, and subhedral to euhedral. The crystals are up to 350 µm long, and equant to elongate, with aspect ratios up to 5:1. In CL images, concentric zoning is ubiquitous (Fig. 6j). Sixteen analyses of 16 zircons are concordant to slightly discordant (Fig. 7j) and yield a weighted mean $^{207}Pb^*/^{206}Pb^*$ date of 2932 ± 5 Ma (MSWD = 0.72), interpreted as the igneous crystallization age.

GSWA 219311: metamonzogranite, Koolanooka Hills

This outcrop sample is a fine- to medium-grained, equigranular, biotite metamonzogranite, consisting of about 35–40% plagioclase, 30% K-feldspar, 25% quartz, 5% biotite, 1–2% myrmekite, 1% magnetite, secondary chlorite or epidote, and trace allanite, titanite, apatite and zircon. The sample lacks a tectonic fabric but has undergone mild solid-state deformation, probably at low to moderate grade, as indicated by residual strain, myrmekite, and microcline twinning.

Zircons from this sample are colourless to dark brown or opaque, subhedral to euhedral, up to 300 µm long, and mainly elongate, with aspect ratios up to 6:1. In CL images, concentric zoning is ubiquitous (Fig. 6k). Eighteen analyses of 18 zircons are concordant to strongly discordant (Fig. 7k). Excluding two analyses >5% discordant, 16 analyses yield a weighted mean $^{207}Pb^*/^{206}Pb^*$ date of 2946 ± 4 Ma (MSWD = 1.3), interpreted as the igneous crystallization age.

GSWA 242652: metavolcanic rock, Koolanooka Hills

This outcrop sample is an altered, fine-grained metavolcanic rock, consisting of about 75% microcrystalline material, 5% actinolitic hornblende, 5% epidote, 5% quartz, 3% biotite, 3% chlorite, 2% carbonate minerals, and trace opaque minerals, sulfide minerals, and prehnite. The sample lacks original volcanic textures but may be a siliceous tuffaceous rock rather than a coherent lava. It has been metamorphosed (probably contact metamorphosed given the rock is not obviously deformed), although the epidote, chlorite, carbonate minerals, and at least some of the quartz, are lower-temperature secondary minerals.

Zircons from this sample are colourless to dark brown and mainly subhedral to euhedral. Concentric zoning is ubiquitous, although about half of the zircons luminesce brightly whereas the others are dark (Fig. 6l). Thirty-six analyses of 30 zircons are concordant to strongly discordant (Fig. 7l), and four analyses >5% discordant are not considered further. Fourteen analyses of 13 mainly low-U zircons (104–542 ppm, median 179 ppm) yield a weighted mean $^{207}Pb^*/^{206}Pb^*$ date of 2961 ± 4 Ma (MSWD = 0.68), interpreted as the igneous crystallization age. Seventeen analyses of 14 mainly high-U zircons (276–703 ppm, median 483 ppm) yield a weighted mean $^{207}Pb^*/^{206}Pb^*$ date of 2994 ± 3 Ma (MSWD = 0.96), interpreted as the age of a xenocrystic component. One analysis yields a $^{207}Pb^*/^{206}Pb^*$ date of 2943 ± 12 Ma (1σ), interpreted to reflect minor loss of radiogenic Pb.

GSWA 242672: felsic metavolcanic rock, Koolanooka Hills

This sample, collected from outcrop in the southern Koolanooka greenstone belt, is a very fine-grained, compositionally layered, felsic metavolcanic rock, consisting of about 20–25% plagioclase, 20–25% K-feldspar, 25% garnet, 20% quartz, 6–7% epidote, 3–4% clinopyroxene, and minor sericite, zircon, apatite and carbonate minerals. The layering is defined mainly by garnet and lenses of quartz, and by subtle differences in grain size. The sample is strongly recrystallized, and the garnet–clinopyroxene–plagioclase–K-feldspar assemblage is consistent with high-grade metamorphism of a fine-grained felsic volcanic protolith.

Zircons from this sample are pale pink to dark red and subhedral to euhedral. The crystals are up to 200 µm long, and equant to slightly elongate, with aspect ratios up to 3:1. In CL images, broad concentric zoning is ubiquitous, and some crystals exhibit narrow, discontinuous rims of luminescent material (Fig. 6m). Seventeen analyses of 17 zircons are concordant to slightly discordant (Fig. 7m) and yield a weighted mean $^{207}Pb^*/^{206}Pb^*$ date of 3002 ± 4 Ma (MSWD = 0.62), interpreted as the igneous crystallization age.

Lutetium–hafnium isotopes

Lu–Hf isotope data for six dated samples from the Gossan Hill Formation, two samples from the Madoonga Formation, three samples from contemporaneous gneisses, and for selected detrital samples are presented in Figure 12 and Table 4 (complete data table is in Appendix 3). This dataset for 3.0 – 2.9 Ga rocks significantly augments previous Hf isotope data for the Youanmi Terrane (Ivanic et al., 2012; Wyche et al., 2012; Mole et al., 2014), which is dominated by 2.8 – 2.6 Ga zircons. Also included are data for a sample of the 2.97 Ga Madoonga Formation (GSWA 193972, Wingate et al., 2012b; Ivanic et al., 2012).

Zircon $\varepsilon_{Hf(i)}$ values for the Gossan Hill Formation are -5.64 to 3.69 and model ages (T_{DM}^2) are 3.74 – 3.15 Ga (Fig. 12a,c; Table 4). Similar results are obtained for the Madoonga Formation but within a narrower range: $\varepsilon_{Hf(i)}$ = -3.55 – 3.10 and T_{DM}^2 = 3.65 – 3.18 Ga. Granitic rocks proximal to the Gossan Hill Formation yield depleted-mantle-like $\varepsilon_{Hf(i)}$ up to 6.67 to CHUR-like 0.53 and slightly older T_{DM}^2 of 3.52 to 3.21 Ga. Detrital zircons from several formations within the Youanmi Terrane indicate depleted ($\varepsilon_{Hf(i)}$ up to 3.05), CHUR-like ($\varepsilon_{Hf(i)}$ = 0.06) and evolved ($\varepsilon Hf_{(i)}$ down to -11.7) isotope signatures with T_{DM}^2 from 4.13 to 3.04 Ga. Two samples from Wyche et al. (2012) provided zircons with distinctly depleted $\varepsilon_{Hf(i)}$ values of 7.30 and 6.75, which plot above the depleted mantle evolution curve. The latter result is within uncertainty of values obtained for the Windimurra Igneous Complex (Nebel et al., 2013), implicating this as a more significant depleted mantle melting event. Detrital zircons from sample 142920 yield Hadean T_{DM}^2 (Fig. 12c).

The average $\varepsilon_{Hf(i)}$ for zircons from the Gossan Hill Formation and the Madoonga Formation is about 0.64 (Fig. 12a), which is close to CHUR values (±0.4). The Thundelarra Supersuite and detrital zircons on Figure 12a are more scattered in terms of age and $\varepsilon_{Hf(i)}$. The negative $\varepsilon_{Hf(i)}$ values for zircons from both of these formations are more restricted (i.e. mostly within the range 0 to -3) than the extremely negative values found in younger zircons in 2.75 to 2.6 Ga rocks from the Youanmi Terrane (i.e. many at -4 to -12; Ivanic et al., 2012). Zircons from the Thundelarra Supersuite are dominantly suprachondritic and have a similar spread of $\varepsilon_{Hf(i)}$ values to these two formations (Fig. 12a,b), whereas 95% of detrital zircons between 3.0 and 2.9 Ga are subchondritic, with a group of grains at extremely negative $\varepsilon_{Hf(i)}$ (-8 to -12).

Volcaniclastic sample 198293, of the Norie Group in the southern Yalgoo–Singleton greenstone belt, has a maximum age of deposition of c. 2826 Ma, and contains a wide spectrum of detrital zircon ages, which define a $\varepsilon_{Hf(i)}$–t trend approaching depleted mantle at 4.2 Ga.

Discussion

Geochronology of volcanic and plutonic rocks

Crystallization ages for the lower three members of the Gossan Hill Formation (GSWA 203701, 203702, 203703 and 203704, Fig. 2, inset) are in good agreement and indicate a weighted mean age of 2961 ± 4 Ma (MSWD = 1.4). The 2947 ± 4 Ma age for the overlying Minjar Member (GSWA 211102), is about 14 Ma younger. The interpreted magmatic crystallization age of 2951 ± 6 Ma for the Gnows Nest Granodiorite (GSWA 207683) suggests the intrusion is a subvolcanic equivalent of the Scuddles Member. However, this age is slightly younger than the c. 2960 Ma dates obtained for the Scuddles Member. Therefore, it is possible that the older 2962 ± 4 Ma metadacite (GSWA 203702) represents an earlier phase of dacitic magmatism within the Scuddles Member.

Although previously thought to be similar in age (Guilliamse, 2014), the Gossan Hill Formation is distinctly younger than the c. 2976 Ma Madoonga Formation (Fig. 11). The Gossan Hill Formation is distinctly older than the c. 2930 Ma Mount Gibson Formation (Yeats et al. 1996). Individually these three successions are assigned as separate formations and are not extensive enough to become a 'group' thus, the 'Mount Gibson Group' (Van Kranendonk et al. 2013) is obsolete.

The felsic metavolcanic rock, GSWA 207670, dated at 2941 ± 3 Ma, from the Edamurta Range provides the only age within greenstones on the western flank of the Yalgoo Dome. Some of the Edamurta greenstone succession is crosscut by the c. 2960 Ma Kynea Migmatite, thus there are likely older components within this succession. The age is within analytical uncertainty of the nearby Edamurta metagranodiorite (GSWA 227224, 2941 ± 3 Ma) and the Perenjori metamonzogranite (GSWA 219311, 2946 ± 4 Ma), located about 100 km to the south in the Koolanooka Hills.

In the southwest of the Yalgoo–Singleton greenstone belt, dates define two distinct felsic magmatic ages in the Koolanooka greenstone belt of c. 3000 and 2960 Ma (GSWA 242672 and 242652, respectively, Fig. 7). At c. 2946 Ma, the age of the Perenjori metamonzogranite within the gneissic dome to the north of the Koolanooka greenstone belt (Fig. 2), is therefore distinctly younger than the dated greenstones.

No mafic intrusions >2.82 Ga have been identified, although several granitic units are thought to have been emplaced at c. 2950 Ma (2955 ± 12 Ma, for five samples proximal to and including the Kynea Migmatite; e.g. Zibra et al., 2018) and these comprise principally metagranodioritic and metatonalitic rocks. These are assigned to the Thundelarra Supersuite based on compositional similarity and a restricted age range.

The 2946 ± 4 Ma Perenjori granodiorite (GSWA 219311; Fig. 2) is similar in age, or slightly younger than, several other intrusions dated at c. 2950 Ma, including the 2960 ± 10 Ma Kynea Migmatite (GSWA 209689, Lu et al., 2017a), the 2945 ± 6 Ma Dromedary Bore Granite (GSWA 198213, Wingate et al., 2015a), the 2950 ± 8 Ma Wurarga Granodiorite (Fletcher and McNaughton, 2002) and the 2964 ±10 Ma Mullewa Granite (Fletcher and McNaughton, 2002). Our samples identify c. 2950 Ma magmatic crystallization ages in felsic plutons that are likely synvolcanic, including the Gnows Nest Granodiorite at Golden Grove, the Great Northern granodiorite at Mount Gibson and the Edamurta Range tonalite in the northwest of the Yalgoo–Singleton greenstone belt. These are within analytical uncertainty of our interpreted magmatic crystallization ages for the Scuddles Member, the Mount Gibson Group and the Edamurta rhyolite, respectively.

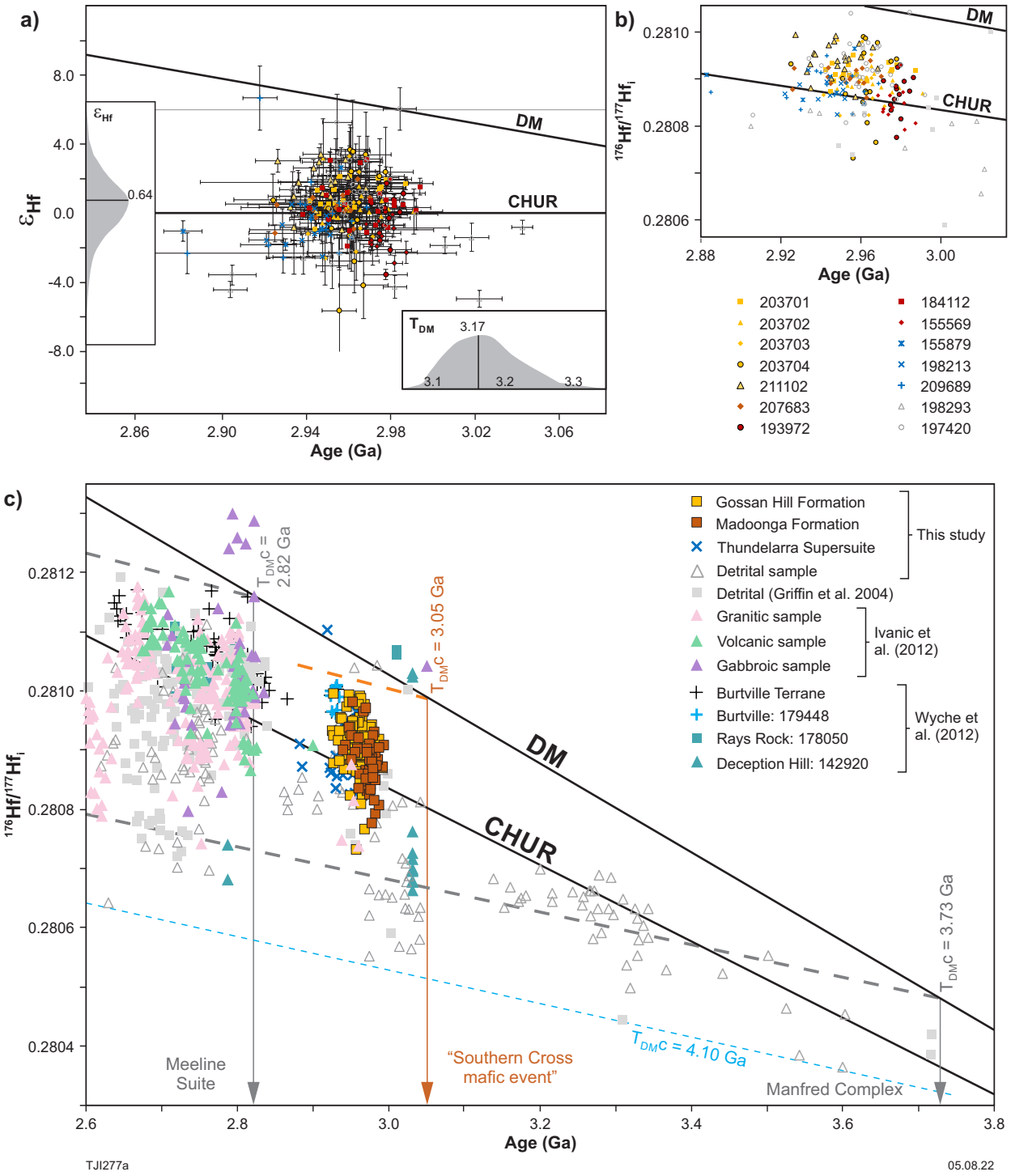

Figure 12. a) Epsilon-Hf vs time plot for Gossan Hill and Madoonga Formations, the Thundelarra Supersuite and detrital samples, error bars are ± 1 sigma; b) initial $^{176}Hf/^{177}Hf$ vs time plot for Gossan Hill Formation samples; c) initial $^{176}Hf/^{177}Hf$ vs time plot for all Youanmi Terrane data (detrital zircon data shown in light grey from Griffin et al., 2004) other samples from Ivanic et al. (2012) and Wyche et al. (2012). The depleted mantle (DM) line was extrapolated from a present DM with $^{176/177}Hf$ of 0.283251 and $^{176}Lu/^{177}Hf$ of 0.0384 (Griffin et al., 2004)

Table 4. Summary of lutetium–hafnium isotope data for selected samples

Sample	*Lithology*	*Lithostratigraphic unit*	*Isotopic age (Ga)*	*No. of analyses*	*εHf (max)*	*εHf (min)*	*T_{DM}^2 max*	*T_{DM}^2 min*
Gossan Hill Fm. (entire)					3.69	-5.64	3.74	3.15
203701	metadacite	Scuddles Mbr/Gossan Hill Fm.	2.96	10	2.19	-0.89	3.42	3.24
203702	metadacite	Scuddles Mbr/Gossan Hill Fm.	2.96	22	3.19	-0.57	3.40	3.17
203703	metarhyolite	Golden Grove Mbr/Gossan Hill Fm.	2.96	7	3.30	-2.59	3.54	3.17
203704	metarhyolite	Gossan Valley Mbr/Gossan Hill Fm.	2.96	21	3.69	-5.64	3.74	3.17
207683	metatonalite	Gnows Nest Granodiorite	2.95	15	1.97	-1.15	3.44	3.26
211102	felsic metavolcaniclastic rock	Minjar Mbr/Gossan Hill Fm.	2.95	24	3.43	-0.97	3.44	3.15
Madoonga Fm. (entire)					3.10	-3.55	3.65	3.18
193972	metarhyolite clast	Madoonga Formation	2.97	18	1.97	-3.55	3.65	3.25
184112	metasandstone	Madoonga Formation	2.97	26	3.10	-1.90	3.50	3.18
155569	metarhyolite	Madoonga Formation	2.97	10	-0.08	-2.89	3.54	3.40
Granitic rocks								
209689	metatonalite	Kynea Migmatite	2.95	15	6.67	-2.57	3.52	3.25
155879	granodiorite gneiss	Kynea Migmatite	2.95	4	2.65	-1.81	3.47	3.21
198213	syenogranite gneiss	Dromedary Bore Granodiorite	2.94	12	0.53	-2.50	3.53	3.33
Selected detrital data								
207686	volcaniclastic metasandstone	Polelle Group	2.79	7	0.60	-5.10	3.66	3.35
197420	metasandstone	Ryansville Formation	2.73	32	3.05	-3.58	3.57	3.04
211101	volcaniclastic mudstone	Mougooderra Formation	2.73	3	0.58	-0.64	3.40	3.34
198293	volcaniclastic metasandstone	Norie Group	2.82	7	0.08	-4.42	3.67	3.37
169066	felsic metavolcanic rock	unassigned	2.73	6	-0.76	-11.66	4.13	3.43
Other rock units								
142920	felsic volcanic rock	unassigned	2.78	13	6.75	-11.38	3.03	-
178050	granodiorite	Tuckanarra Suite	2.71	2	7.30	6.42	3.03	3.03
198212	monzogranite	Walganna Suite	2.67	2	0.18	-0.41	3.40	3.36

The Gossan Hill and Madoonga Formations

The Gossan Hill Formation is interpreted to represent a felsic volcanic centre, consisting of three members erupted at c. 2961 Ma, followed by the dominantly siliciclastic Minjar Member at c. 2947 Ma. Basaltic lavas of the Polelle Group are interpreted to unconformably overlie the formation, although the contact is not exposed. The Gossan Hill Formation is not clearly associated with basaltic magmatism and is interpreted to have formed from isolated crustal melts. There is a possible link between these magmas and contemporaneous migmatitic events at depth (e.g. Kynea Migmatite, Zibra et al. 2020), which is similar in age to the Gossan Hill Formation.

We interpret the Gnows Nest Granodiorite and porphyritic dacitic dykes as a comagmatic, subvolcanic magmatic system, which fed lavas of the Scuddles Member. In detail, this is because: (1) the age and εHf of the Gnows Nest Granodiorite is within analytical uncertainty of results for the Scuddles Member; (2) the Gnows Nest Granodiorite, porphyritic dacitic dykes and porphyritic dacitic lava of the Scuddles Member have similar mineralogy and phenocryst contents; (3) the major and trace-element composition of the Gnows Nest Granodiorite and lavas of the Scuddles Member (chemical group 1) match closely (Fig. 10); and (4) porphyritic dacitic dykes intrude mostly within the Golden Grove and Gossan Valley Members, which magmatically link the Gnows Nest Granodiorite to the base of Scuddles Member lava flows.

We reclassify the stratigraphy of the Golden Grove succession from formation level-units to member-level units. For example, the 'Golden Grove Formation' (Clifford, 1992) becomes the Golden Grove Member and the 'Gossan Hill Group' (Clifford, 1992) becomes the Gossan Hill Formation (Table 1). The 'Cattle Well Formation' has been renamed as the Minjar Member and the 'Shadow Well Formation' has become obsolete as it is thought to have been misidentified as a metasedimentary package but it appears to be locally schistose granodiorite.

The two magmatic ages within the Gossan Hill Formation (2961 ± 3 and 2947 ± 4 Ma) are significantly different. This is a feature shared with the Madoonga Formation (3002 ± 2 and 2975 ± 8 Ma) and Annabelle Volcanics (2989 ± 7 and 2958 ± 4 Ma) and the Koolanooka greenstones (3002 ± 4 and 2961 ± 4 Ma). This may indicate more prolonged and widespread felsic magmatism throughout the 3.0 – 2.9 Ga period than previously thought (Fig. 11, age spectra). These ages, together with the isolated nature of all the formations, led to our assignment of them to the Southern Cross Supergroup, rather than to the Murchison Supergroup.

Using SHRIMP U–Th–Pb monazite dating, Duuring et al. (2019) proposed that banded iron-formation (BIF) in the Weld Range immediately to the south of the Madoonga Formation was deposited at c. 2857 Ma but is possibly older. Thus, this BIF may in fact be the top of the felsic volcanic succession and may represent a long period of deposition and relative quiescence within the 2920–2825 Ma magmatic hiatus (Fig. 3). Furthermore, several undated BIF deposits at Koolanooka, Tallering, Twin Peaks, Mount Gibson and Ravensthorpe (Chester Formation) (see Fig. 4), might also be similar in age to the basal Weld Range BIF.

Geochemistry and petrogenesis

Our data show only limited geochemical trends in volcanic rocks because there are no mafic end members and, given the significant and unknown effects of hydrothermal alteration in the Golden Grove and Weld Range areas, it is difficult to interpret whether they were derived from melts of crust or mantle (or both). The Kynea Migmatite TTG gneisses have compositions and trace-element patterns that we attribute to melting in garnet- or hornblende-bearing lower-crustal sources (cf. Clos et al., 2018). Thinned lithosphere and higher crustal heat flow associated with rifting at 3.0 – 2.9 Ga would account for both lower- and mid-crustal melting. However, in the absence of mafic end-member samples, we cannot assess the degree of mantle input in this time interval. Further study of stratigraphically equivalent magmatic rocks throughout the broader Youanmi Terrane is required to shed more light on the magmatic sources and to provide robust geochemical evidence for the tectonic setting and geodynamic processes operating during this magmatic interval.

Yilgarn Craton correlations

New geochronology presented here significantly adds to the understanding of the older magmatism and greenstone development in the western Yilgarn Craton. Figure 1b shows that geographic links in rocks known to have to have formed between 3.0 and 2.9 Ga extend across most of the western and southern Youanmi Terrane (orange polygon). Further west, there is a distinct, arcuate distribution of >3.0 Ga ages in the westernmost Youanmi Terrane and the Narryer Terrane (red polygon, Fig. 1b). Quentin de Gromard et al. (2021) appraised geochronology among many other lines of evidence, which indicated that rocks of the Youanmi Terrane extended approximately 200 km further west of the previous boundary with the South West Terrane. More work is required to test how the >3.0 Ga rocks relate to the 3.0 – 2.9 Ga rocks and how many distinct terranes comprise the western Yilgarn Craton.

The geometry of the 3.0 – 2.9 Ga rocks is closely coincident with c. 3.3 Ga basement signal in Nd isotope model-age map (Fig. 1c), which is in an arcuate distribution around the Cue Isotopic Zone in the northern Youanmi Terrane. In the southern Youanmi Terrane, Mole et al. (2019) proposed an east–west orientation of a 2.95 Ga rift based upon Hf isotope data and, using whole-rock geochemical data on granitic rocks, Smithies et al. (2018a) also proposed a northeast trending basement heterogeneity in this region based upon interpreted depth of melting for granitic rocks. The gap in c. 3.0 Ga magmatic ages between Wongan Hills and Ravensthorpe (Fig. 1b) may be partly due to lack of sampling in greenstones in these areas, however, the 3.3 Ga Nd isotopic signature is clearly disturbed (i.e. diluted) to younger model ages along this east–west orientation. Thus, it is possible that a northwest-trending corridor of magmatism between 3.01 and 2.91 Ga from Ravensthorpe to Wongan Hills existed and was later overprinted by more east–west trending corridors of mantle-derived magmas. Crustal-scale heterogeneities across this east–west trending overprint could have been the result of known significant tectonic activity and addition of isotopically juvenile material into the Youanmi Terrane crust between 2.8 and 2.7 Ga.

Recent geological mapping (GSWA, 2020) shows the re-interpretation of high-Mg basaltic rocks of the Sandstone greenstone belt, which were assigned to the c. 2.8 Ga Polelle Group, rather than a northerly extension to a komatiite event at c. 2.9 Ga, as suggested previously (Perring et al., 1995; Wang et al., 1996). Similarly, undated boninitic rocks in the Koolyanobbing belt (Angerer et al. 2013), originally interpreted to be c. 3.0 Ga, may correlate with c. 2.8 Ga units identified further north and south. Thus, several studies highlight that the komatiite-bearing, north-trending, 2.95 Ga Ravensthorpe–Sandstone belt may in fact be younger and that the trend of c. 2.95 Ga associations is northwesterly rather than northerly. The continuity of 3.0 – 2.9 Ga crust prior to its modification and its relationship to granites and greenstones >200 km to the northwest is unknown, however.

A magmatic crystallization age of 3023 ± 10 Ma (Fig. 1b, red star symbol with 'x') interpreted for a quartz–feldspar porphyry at Deception Hill in the eastern Youanmi Terrane (GSWA 142920, Nelson, 1999) has a younger age component at c. 2787 Ma, interpreted as Pb-loss. We, consider the c. 3 Ga zircons as xenocrystic in this sample. Another sample dated at 2945 ± 6 Ma, (GSWA 198213; Wingate et al., 2015a, Fig. 1b yellow star symbol with 'x') is interpreted as a raft within a younger granitic gneiss, thus these >2.9 Ga ages within the central Youanmi Terrane are related to the basement, and the axis of > 2.9 Ga volcanism lies further west (Fig. 1b).

The absence of 3.0 – 2.9 Ga formations in the central and northern Youanmi Terrane is interpreted to be a result of voluminous 2.80 – 2.72 Ga magmatism that obscured evidence of these rocks. For example, even in the more extensive stratigraphy of the Southern Cross Supersuite, felsic volcanic rocks in the Gossan Hill and Madoonga Formations are inundated by voluminous crosscutting gabbroic rocks of the Warriedar Suite. However, ubiquitous 3.0 – 2.9 Ga xenocrystic zircons across the Youanmi Terrane indicate that some TTGs and some felsic volcanic rocks are likely widely present at depth in the central and northern portions of the terrane (cf. Ameen and Wilde, 2018).

There is a notable absence of xenocrystic grains in magmatic rocks in this study (i.e. age components >3.01 Ga). This indicates that older basement was systematically not sampled by these magmatic systems and may implicate a thin crust at the time of formation.

Isotopic constraints

Hafnium isotope data from zircons in the Gossan Hill and Madoonga Formations and proximal, synvolcanic TTGs yield a unimodal, homogenous εHf over 40 Ma, indistinguishable from CHUR and with no significant crustal contamination implicated (Fig. 12). Distal TTG gneisses are slightly more evolved, with εHf(i) between 0 and -2, indicating minor contributions from a >3.3 Ga crustal component. The mantle source for these units is interpreted to be primitive mantle and a rift setting is consistent with persistent and homogenous Hf isotope compositions through time and space.

Wyche et al. (2012) present Hf data from samples across the eastern Youanmi Terrane and Eastern Goldfields Superterrane and highlight three distinct periods of crustal growth and recycling – at or before c. 4.2, 3.5, and 3.1 Ga. Here, we show that 3.0 – 2.9 Ga TTGs in the Youanmi Terrane are closely linked with several phases of coeval volcanic rocks, locally with similar chemical compositions to TTGs. The range of Hf isotope compositions in zircons from these rocks indicates a similar juvenile source with limited recycling of 3.5 – 3.2 Ga basement. Thus, we interpret this phase of magmatism to represent rift-related crust formation driven locally by thermal effects distal to a plume.

In detrital sample GSWA 198293, we interpret its recycling εHf–t trend from 4.1 to 2.8 Ga (approaching depleted mantle at 4.1 Ga) as exposure of zircon-crystallizing rocks with Narryer Terrane ages in the detrital source region(s). Detrital components within sediments that have been reworked into this rock might alternatively have been derived from exposure of magmatic rocks of the Narryer Terrane. The trend also indicates that punctuated magmatism in the Youanmi Terrane has consistently involved recycling of Eoarchean–Hadean basement at c. 3.34, 3.32, 3.29, 3.27, 3.20, 3.17, 3.04, 3.02, 2.96, 2.94, 2.90 and 2.89 Ga (cf. Ivanic et al., 2012), over ~500 million years.

The Cue Isotopic Zone (CIZ) is juxtaposed slightly to the east of c. 2.95 Ga formations in the northern Youanmi Terrane. If this juvenile zone was caused by a rift, then axial subsidence would have thinned and taken old basement rocks to deeper levels, to be covered extensively by 2.82 – 2.72 Ga volcanic rocks of the Norie, Polelle and Glen Groups — in this way, a rift could account for the absence of 3.01 – 2.92 Ga rocks in the western part of the CIZ. Rocks with older Nd model ages to the east and west of the 3.01 – 2.92 Ga formations (Fig. 1c) are indicative of the recycling of Narryer-age crust at depth (Ivanic et al., 2012; Wyche et al., 2012). A narrow juvenile zone transecting the Yilgarn Craton is consistent with a large-scale and long-lived rift setting. In this scenario, crustal thinning must have progressed sufficiently to allow significant mafic input into the greenstone successions such as the Madoonga and Mount Gibson Formations and minor amounts into the other successions. The limited amount of geochemical and isotope data available is insufficient to completely rule out input from metasomatized mantle or even a mantle plume during this time interval.

Craton-wide considerations

The Illara–Maynard Hills greenstone belt hosts metasedimentary rocks with abundant 3.6 – 3.0 Ga, and some 4.3 – 3.6 Ga zircons (Nelson, 2002; Wyche, 2007). Thern and Nelson (2012) infer a maximum age of deposition in these belts of c. 3.06 Ga, and a minimum age from a Mount Alfred locality of c. 2.94 Ga (Thern et al., 2011; 2020; about 50 km north of the red star with 'x' in Fig. 1b). Since no magmatic rocks of this age have been identified in the eastern part of the Youanmi Terrane, these metasedimentary successions are likely coeval depocentres, distal to the felsic volcanic centres further west at c. 2.95 Ga. Thus, the rift axis may have been located along the juvenile isotopic zone (Fig. 1c) with an eastward paleocurrent direction.

The Eastern Goldfields Superterrane hosts limited magmatic rocks older than 2.9 Ga (Fig. 11), including the Penneshaw Formation (Kositcin et al., 2008), dacite from the Merolia Domain of the Burtville Terrane and three granodiorites from the northern Kurnalpi Terrane. The distribution of these rocks within the craton is shown on Figure 1b and may have been craton-wide (>800 km in extent). The voluminous magmatic

input during the Kalgoorlie rift event may be responsible for the near absence of older rocks in the east-central Yilgarn Craton.

Studies of VHMS deposits in the Yilgarn Craton link >2.9 Ga greenstone belts at Golden Grove, Weld Range, and Ravensthorpe (e.g. Hollis et al., 2015; Guilliamse, 2014). However, we show that at least 10 formations likely form a chain of individual volcanic centres. Their trend along a northwest-trending corridor next to juvenile isotopic signatures in the CIZ in the northern part of the terrane, leads to our interpretation of these formations as localized magmatic events along a long-lived (~100 Ma) rift zone. This interpretation is consistent with 'rift-related volcanism' invoked for the Golden Grove succession (Clifford, 1992; Sharpe and Gemmell, 2001), in which synvolcanic normal faults have been identified. However, it also remains a possibility that this linear magmatic belt is related to subduction processes, although evidence of thrust tectonics is not currently reported. Additional geochemical studies on these rocks are likely to shed more light on the evolution of this interval in Youanmi Terrane history.

The relatively narrow range of mostly suprachondritic εHf values in felsic volcanic and intermediate gneisses within 3.0 – 2.9 Ga rocks of the Youanmi Terrane suggests that there was limited prolonged juvenile input and limited recycling at this time. Similar to the post-2.9 Ga rocks of the Youanmi Terrane (Ivanic et al., 2012), Hf data suggest limited recycling of 3.8 – 3.1 Ga crust in a small number of samples. Thus, lower-crustal basement was likely well established over a wide area by 3.0 Ga (the Eo-Paleoarchean Yilgarn protocraton), enabling widespread and sporadic rift-related magmatism from 3.0 to 2.9 Ga.

There is a distinct lack of xenocrystic zircons in magmatic rocks in this study and all but one volcanic sample yield unimodal magmatic zircon populations. This feature is also noted in previous work on correlative rocks (e.g. GSWA 112163, Nelson, 1995a). We consider this to reflect a paucity of basement during 3.0 – 2.9 Ga magmatism, which may indicate a thin crust from c. 3 Ga.

Implications for mineralization

Linking 3.01 – 2.92 Ga stratigraphic units lithologically and geochemically in domains across the Yilgarn Craton widens the exploration potential for Au and VHMS deposits. These correlations not only provide geographic control but also document the extent and thickness of ore-associated formations and suites (Table 3). Through time there is no particular pattern to the types of deposits except that most major polymetallic VHMS deposits occur between 2.96 and 2.94 Ga. Copper and gold are ubiquitous (but with variable size) across the 3.01 – 2.92 Ga corridor in the Youanmi Terrane. Synvolcanic plutons rarely host mineralization and, where they do, it is dominantly gold.

The flanks of the CIZ, interpreted as the edges of a rift, are believed to have been exploited by mineralizing fluids in formation of the Golden Grove deposit. Thus, other units of comparable age in a similar location would be considered to have had the appropriate geodynamic setting for similar deposits to have formed. The identification of 3.01 – 2.92 Ga felsic volcanic centres across a >700 km expanse of the western Yilgarn Craton (possibly craton-wide), opens up a large potential exploration space for VHMS deposits.

The global Mesoarchean record

Puchtel et al. (1999) described komatiite-bearing greenstones from the southeastern Baltic Shield with units dated imprecisely at c. 2.9 Ga. Mafic–ultramafic lavas and basalt–andesite–dacite–rhyolite (BADR) lavas yielded εNd of about +2.5 and the BADR lavas are characterized by large negative HFSE (and Nb) anomalies. The authors attributed formation of the greenstone package to mantle plume or island arc processes. Similarly, Hollings and Wyman (1999) described well-dated 3.0 Ga volcanic rocks, which include komatiites, from the western Superior Province in Ontario. Rhyolites from this succession have HREE-depleted and HREE-enriched patterns interpreted to represent diverse sources and yielded a hypothesis of a plume impinging on an arc or a cratonic nucleus.

The Fiskenaesset Complex (a dismembered mafic–ultramafic layered intrusion) in western Greenland is dated at 2945 Ma with εNd = +3.3 (Polat et al., 2010). These authors attribute its tectonic setting to an island arc based on trace-element chemistry, specifically the variable REE patterns from depleted to enriched to concave-up (Polat et al., 2009). In the Pilbara Craton, several magmatic units have been identified at c. 2.9 Ga. In the west Pilbara, the Munni Munni Complex (a layered mafic–ultramafic intrusion), dated at 2925 Ma (GSWA 178165, Wingate et al., 2012a) is interpreted to have formed from komatiitic and tholeiitic melts (Barnes and Hoatson, 1994). Granitic intrusions spanned the east and the west Pilbara Craton during this interval, but volcanic activity was focused in the Mallina Basin at c. 2.95 Ga. Some of these rocks are interpreted to have boninitic affinity (Smithies et al., 2005).

Using geochemical signatures in Archean basalts from Western Australia, Smithies et al. (2018a) highlights 3.10 – 2.75 Ga as a period of subduction initiation or failed subduction, with plume-dominant geodynamics prevalent before 3.1 Ga and at 2.7 Ga. The global magmatic record from 3.1 – 2.9 Ga is typically bimodal, with komatiitic and BADR melts. Komatiitic rocks are interpreted as plume-related and BADR rocks locally show variably strong geochemical evidence for input from a metasomatized mantle source.

Thus, our data and interpretation of a rift setting may fit with some of the above-mentioned tectonic models derived from cratons worldwide during this period. However, in this time bracket obvious plume-related or subduction-related rocks are currently either not present or not sampled within the Youanmi Terrane.

Conclusions

Ten 3.01 – 2.92 Ga stratigraphic units consisting of mostly felsic volcanic rocks extend in a >750 km long corridor in the western and southern Youanmi Terrane. In the south, these are spatially associated with (undated) komatiite lava units. The VHMS-hosting Gossan Hill Formation has been divided into four members and is comagmatic with one granodiorite intrusion of the Thundelarra Supersuite (Gnows Nest Granodiorite). Our main findings from the Gossan Hill Formation are that:

1. The lower, mineralized part of the formation, consisting of three members, was probably deposited within 4 Ma and represents a large but isolated volcanic centre at c. 2960 Ma.

2. The Gossan Hill Formation shows lithological, chemical and isotopic similarity to the older Madoonga Formation and several other felsic volcanic-bearing formations in the southern Youanmi Terrane. The Annabelle Volcanics to the far south and several TTG gneisses proximal to the Gossan Hill Formation yield similar magmatic crystallization ages to the Gossan Hill Formation.

Yilgarn-wide conclusions are as follows:

1. Thirteen geochronology samples in this report place constraints on a widespread magmatic episode from 3.01 to 2.92 Ga, involving the Southern Cross Supergroup and Thundelarra Supersuite.

2. The Southern Cross Supergroup extends in a north-northwest trending corridor (Fig. 1b, orange polygon) in the western Youanmi Terrane. There is a possibility that this once crossed the entire (>750 km) of the terrane. There is also a less well-constrained, north-trending corridor of similar age in the eastern Youanmi Terrane. Rocks of the Southern Cross Supergroup and the Thundelarra Supersuite are located around the CIZ, in an arcuate distribution, mirroring the regions of c. 3.3 Ga model ages on the Nd isotope model-age map (Fig. 1c).

3. The magmatism typically involves felsic volcanic rocks and subvolcanic intrusions within greenstone belts, which are locally dominated by mafic volcanic rocks. The Thundelarra Supersuite of TTG gneisses is distal to greenstone belts and not necessarily representative of older basement. Locally abundant mafic volcanic rocks are associated with dated felsic volcanic rocks within many of these greenstone belts, although there is poor age control on them or on the mafic intrusions within these belts.

4. Paucity of xenocrystic zircons in the geochronology samples may be a result of limited sampling of basement material by these magmas and the presence of a thinned (and possibly rifted) crust at about 3.01 Ga.

5. Zircon lutetium–hafnium isotope data from the Gossan Hill and Madoonga Formations indicate that limited older 3.4 – 3.1 Ga crust was recycled, and the dominant magmatic input into the crust was juvenile. Detrital zircon samples indicate that depleted mantle input as well as recycling of up to 3.8 Ga crust likely occurred between 3.1 and 2.9 Ga.

6. The 3.01 – 2.92 Ga formations and associated TTGs formed a large component of the upper crust of the Youanmi Terrane. This magmatism culminated in a protocratonic stage of the Yilgarn Craton at 2.9 Ga, followed by a hiatus of 0.1 Ga.

7. We interpret this magmatism to be rift-related, however, mantle plume activity cannot be ruled out and more geochemical data will also test whether any metasomatized mantle sources were present.

8. Additional work is required to constrain the full extent and duration of 3.01 – 2.92 Ga events within the Yilgarn Craton and to determine the petrogenesis and tectonic setting for magmatic rocks during this time interval.

References

Ameen, SM and Wilde, SA 2018, Multiple sources for Archean granitoids in the Yalgoo area, Yilgarn Craton, Western Australia: Geochemical and isotopic evidence: Precambrian Research, v. 314, p. 76–110.

Angerer, T, Kerrich, R and Hagemann, SG 2013, Geochemistry of a komatiitic, boninitic, and tholeiitic basalt association in the Mesoarchean Koolyanobbing greenstone belt, Southern Cross Domain, Yilgarn craton: Implications for mantle sources and geodynamic setting of banded iron formation: Precambrian Research, v. 224, p. 110–128.

Barnes, SJ and Hoatson, DM 1994, The Munni Munni Complex, Western Australia: Stratigraphy, Structure and Petrogenesis: Journal of Petrology, v. 35, p. 715–751.

Bouvier, A, Vervoort, JD and Patchett, PJ 2008, The Lu–Hf and Sm–Nd isotopic composition of CHUR: constraints from unequilibrated chondrites and implications for the bulk composition of terrestrial planets: Earth and Planetary Science Letters, v. 273, no. 1–2, p. 48–57, doi:10.1016/j.epsl.2008.06.010.

Cassidy, KF, Champion, DC, McNaughton, NJ, Fletcher, IR, Whitaker, AJ, Bastrakova, IV and Budd, A (editors) 2002, The characterisation and metallogenic significance of Archaean granitoids of the Yilgarn Craton, Western Australia: Minerals and Energy Research Institute of Western Australia, MERIWA Project no. M281/AMIRA Project no. 482 (Report No. 222).

Cassidy, KF, Champion, DC, Krapez, B, Barley, ME, Brown, SJA, Blewett, RS, Groenewald, PB and Tyler, IM 2006, A revised geological framework for the Yilgarn Craton, Western Australia: Geological Survey of Western Australia, Record 2006/8.

Clifford, BA 1992, Facies and palaeoenvironment analysis of the Archaean volcanic-sedimentary succession hosting the Golden Grove Cu-Zn massive sulphide deposits, Western Australia: Monash University, PhD thesis (unpublished), 343p.

Clos, F, Weinberg, RF and Zibra, I 2018, Building the Archean continental crust: 300 Ma of felsic magmatism in the Yalgoo dome (Yilgarn Craton): Geological Survey of Western Australia, Report 186, 23p.

Dalstra, HJ 1995, Metamorphic and structural evolution of greenstone belts of the Southern Cross - Diemals region of the Yilgarn Block, Western Australia, and its relationship to gold mineralisation: The University of Western Australia, Perth, PhD thesis (unpublished), 219p.

DeBievre, P and Taylor, PDP 1993, IUPAC Recommended Isotopic Abundances: International Journal of Mass Spectrometry and Ion Physics, v. 123, p. 149.

Dunphy, JM, Fletcher, IR, Cassidy, KF and Champion, DC 2003, Compilation of SHRIMP U-Pb geochronological data, Yilgarn Craton, Western Australia, 2001-2002: Geoscience Australia, Record 2003/15, 139p.

Duuring, P, Santos, JOS, Fielding, IOH, Ivanic, TJ, Hagemann, SG, Angerer, T, Lu, Y-J, Roberts, M and Choi, J 2020, Dating hypogene iron mineralization events in Archean BIF at Weld Range, Western Australia: insights into the tectonomagmatic history of the northern margin of the Yilgarn Craton: Mineralium Deposita, v. 55, doi:10.1007/s00126-019-00930-3

Eggins, SM, Woodhead, JD, Kinsley, LPJ, Mortimer, GE, Sylvester, PJ, McCulloch, MT, Hergt, JM and Handler, MR 1997, A simple method for the precise determination of >40 trace elements in geological samples by ICPMS using enriched isotope internal standardisation: Chemical Geology, v. 134, p. 311–326.

Elliott, BA 2018, Petrogenesis of heavy rare earth element enriched rhyolite: source and magmatic evolution of the Round Top Laccolith, Trans-Pecos, Texas: Minerals, v. 8, p. 423, doi:10.3390/min8100423

Fletcher, IR and McNaughton, NJ 2002, Chapter 6. Granitoid geochronology: SHRIMP zircon and titanite data, *in* The characterisation and metallogenic significance of Archaean granitoids of the Yilgarn Craton, Western Australia *edited by* KF Cassidy, DC Champion, NJ McNaughton, IR Fletcher, AJ Whitaker, IV Bastrakova and A Budd: Minerals and Energy Research Institute of Western Australia, MERIWA Project no. M281/AMIRA Project no. 482 (Report No. 222), p. 6.1–6.156.

Foley, BJ 1997, Reassessment of Archaean tectonics in the Yalgoo District, Murchison Province, Western Australia: Monash University, Melbourne, Australia, BSc thesis (unpublished), 86p.

Frater, KM 1983, Geology of the Golden Grove prospect, Western Australia: A volcanogenic massive sulfide-magnetite deposit: Economic Geology, v. 78, p. 875–919.

Gee, RD 1980, Summary of Precambrian stratigraphy of Western Australia, in Annual report for the year 1979: Geological Survey of Western Australia, Perth, Western Australia, p. 85–90.

Geological Survey of Western Australia 2020, Youanmi, 2020: Geological Survey of Western Australia, Geological Information Series.

Geological Survey of Western Australia 2021, WAROX, 2021: Geological Survey of Western Australia, Geological Information Series.

Geoscience Australia and Australian Stratigraphy Commission 2020, Australian Stratigraphic Units Database, viewed 15 January 2020, <https://asud.ga.gov.au/search-stratigraphic-units/>.

Griffin, WL, Pearson, NJ, Belousova, EA, Jackson, SE, O'Reilly, SY, van Achterbergh, E and Shee, SR 2000, The Hf isotope composition of cratonic mantle: LAM-MC-ICPMS analysis of zircon megacrysts in kimberlites: Geochimica et Cosmochimica Acta, v. 64, no. 1, p. 133–147.

Griffin, WL, Belousova, EA, Shee, SR, Pearson, NJ and O'Reilly, SY 2004, Archean crustal evolution in the northern Yilgarn Craton: U-Pb and Hf-isotope evidence from detrital zircons: Precambrian Research, v. 131, p. 231–282.

Guilliamse, J 2014, Assessing the potential for volcanic-associated massive sulfide mineralization at Weld Range, using Golden Grove for comparison: Geological Survey of Western Australia, Report 141, 61p.

Hollings, P and Wyman, DA 1999, Trace element and Sm–Nd systematics of volcanic and intrusive rocks from the 3 Ga Lumby Lake Greenstone belt, Superior Province: evidence for Archean plume–arc interaction: Lithos, v. 46, p. 189–213.

Hollis, SP, Yeats, CJ, Wyche, S, Barnes, SJ, Ivanic, TJ, Belford, SM, Davidson, GJ, Roache, AJ and Wingate, MTD 2015, A review of volcanic-hosted massive sulfide (VHMS) mineralization in the Archaean Yilgarn Craton, Western Australia: tectonic, stratigraphic and geochemical associations: Precambrian Research, v. 260, p. 113–135, doi:10.1016/j.precamres.2014.11.002.

Ivanic, TJ 2019, Mafic–ultramafic intrusions of the Youanmi Terrane, Yilgarn Craton: Geological Survey of Western Australia, Report 192, 130p.

Ivanic, TJ, Wingate, MTD, Kirkland, CL, Van Kranendonk, MJ and Wyche, S 2010, Age and significance of voluminous mafic-ultramafic magmatic events in the Murchison Domain, Yilgarn Craton: Australian Journal of Earth Sciences, v. 57, p. 597–614.

Ivanic, TJ, Van Kranendonk, MJ, Kirkland, CL, Wyche, S, Wingate, MTD and Belousova, E 2012, Zircon Lu-Hf isotopes and granite geochemistry of the Murchison Domain of the Yilgarn Craton: Evidence for reworking of Eoarchean crust during Meso-Neoarchean plume-driven magmatism: Lithos, v. 148, p. 112–127.

Ivanic, TJ, Van Kranendonk, MJ, Kirkland, CL, Wyche, S, Wingate, MTD and Belousova, EA 2013, Juvenile crust formation and recycling in the northern Murchison Domain, Yilgarn Craton: Evidence from Hf isotopes and granite geochemistry: Geological Survey of Western Australia, Report 120, 34p.

Kennedy, G and Lane, S 2001, Annual Report for the Period 20/8/00 to 19/8/2001: Anglo American.

Korsch, RJ, Blewett, RS, Wyche, S, Zibra, I, Ivanic, TJ, Doublier, MJ, Romano, SS, Pawley, MJ, Johnson, SP, Van Kranendonk, MJ, Jones, LEA, Kositcin, N, Gessner, K, Hall, CE, Chen, SF, Patison, N, Kennett, BLN, Jones, T, Goodwin, JA, Milligan, P and Costelloe, RD 2014, Geodynamic implications of the Youanmi and Southern Carnarvon deep seismic relection surveys: a ~1300 km traverse from the Pinjarra Orogen to the eastern Yilgarn craton, *in* Youanmi and southern Carnarvon seismic and magnetotelluric (MT) workshop 2013 *edited by* S Wyche, TJ Ivanic and I Zibra: Geological Survey of Western Australia, Record 2013/6, p. 147–166.

Kositcin, N, Brown, SJA, Barley, ME, Krapež, B, Cassidy, KF and Champion, DC 2008, SHRIMP U-Pb zircon age constraints on the Late Archaean tectonostratigraphic architecture of the Eastern Goldfields Superterrane, Yilgarn Craton, Western Australia: Precambrian Research, v. 161, p. 5–33.

Le Maitre, RW, Bateman, P, Dudek, A, Keller, J, Lameyre, J, Le Bas, MH, Sabine, PA, Schmid, R, Sorensen, H, Streckeisen, A, Woolley, AR and Zanettin, B 1989, A classification of igneous rocks and glossary of terms: Recommendations of the International Union of Geological Sciences Subcommision on the Systematics of Igneous Rocks: Balckwell Scientific, Oxford, 254p.

Lesher, CM, Goodwin, AM, Campbell, IH and Gorton, MP 1986, Trace-element geochemistry of ore-associated and barren, felsic metavolcanic rocks in the Superior Province, Canada: Candian Journal of Earth Sciences, v. 23, no. 2, p. 222–237.

Lu, Y, Wingate, MTD, Champion, DC, Smithies, RH, Johnson, SP, Mole, DR, Poujol, M, Zhao, J, Maas, R and Creaser RA 2021, Samarium–neodymium isotope map of Western Australia: Geological Survey of Western Australia, digital data layer, <www.dmirs.wa.gov.au/geoview>.

Lu, Y, Wingate, MTD, Kirkland, CL and Ivanic, TJ 2016, 211102: felsic volcaniclastic rock, Mougooderra Hill; Geochronology Record 1338: Geological Survey of Western Australia, 4p.

Lu, Y, Wingate, MTD, Kirkland, CL and Zibra, I 2017a, 209689: metatonalite, Wooley Spring; Geochronology Record 1463: Geological Survey of Western Australia, 4p.

Lu, Y, Wingate, MTD and Kirkland, CL 2017b, 199022: metasyenogranite, Corinthia mine; Geochronology Record 1423: Geological Survey of Western Australia, 4p.

Lu, Y, Wingate, MTD, Thorne, AM and Blay, O 2017c, 216142: granite gneiss, Lawson Well; Geochronology Record 1430: Geological Survey of Western Australia, 4p.

Lu, Y, Wingate, MTD and Kirkland, CL 2018, 203701: metadacite, Cattle Well; Geochronology Record 1495: Geological Survey of Western Australia, 4p.

Lu, Y, Wingate, MTD and Smithies, RH 2019, 224351: metamonzogranite, Woolshed Road; Geochronology Record 1585: Geological Survey of Western Australia, 5p.

Ludwig, KR 2001, SQUID 2.22: A user's manual: Berkeley Geochronology Center, Special Publication 2, 16p.

Ludwig, KR 2003, Isoplot 3.00; a geochronological toolkit for Microsoft Excel: Berkeley Geochronology Centre, Special Publication 4, 70p.

McDonough, WF and Sun, S-S 1995, The composition of the Earth: Chemical Geology, v. 120, p. 223–253.

Middlemost, EA 1994, Naming materials in the magma/igneous rock system: Earth-Science Reviews, v. 37, no. 3, p. 215–224, doi:10.1016/0012-8252(94)90029-9.

MMG Golden Grove Pty Ltd 2014, Golden Grove delivers strong production in 2013, <www.mmg.com/media-release/golden-grove-delivers-strong-production-in-2013-d86/>.

Mole, DR, Fiorentini, ML, Thebaud, N, Cassidy, KF, McCuaig, TC, Kirkland, CL, Romano, SS, Doublier, MP, Belousova, EA, Barnes, SJ and Miller, J 2014, Archean komatiite volcanism controlled by the evolution of early continents: Proceedings of the National Academy of Sciences of the Unites States of America, v. 111, no. 28, p. 10083– 10088.

Mole, DR, Kirkland, CL, Fiorentini, ML, Barnes, SJ, Cassidy, KF, Issac, C, Belousova, EA, Hartnady, M and Thebaud, N 2019, Time-space evolution of an Archean craton: A Hf-isotope window into continent formation: Earth-Science Reviews.

Nebel, O, Arculus, RJ, Ivanic, TJ and Nebel-Jacobsen, YJ 2013, Lu-Hf isotopic memory of plume-lithosphere interaction in the source of layered mafic intrusions, Windimurra Igneous Complex, Yilgarn Craton, Australia: Earth and Planetary Science Letters, v. 380, p. 151–161.

Nelson, DR 1995a, 112163: rhyolite, Bandalup; Geochronology Record 490: Geological Survey of Western Australia, 4p.

Nelson, DR 1995a, 104963: biotite rhyolite, Penneshaw Formation; Geochronology Record 21: Geological Survey of Western Australia, 5p.

Nelson, DR 1996, 105002: dark inclusion phase in orthogneiss, east of Cargarra Well; Geochronology Record 7: Geological Survey of Western Australia, 4p.

Nelson, DR 1999, 142920: quartz–feldspar porphyry, Deception Hill; Geochronology Record 342: Geological Survey of Western Australia, 4p.

Nelson, DR 2000, 142986: metasandstone, Eranondoo Hill; Geochronology Record 289: Geological Survey of Western Australia, 4p.

Nelson, DR 2002, 169074: quartzite, Kohler Bore; Geochronology Record 110: Geological Survey of Western Australia, 4p.

Norrish, K and Chappell, BW 1977, X-ray fluorescence spectrometry, *in* Physical methods in determinative mineralogy *edited by* J Zussman: Academic Press, London, UK, p. 201–272.

Nutman, AP, Bennett, VC, Kinny, PD and Price, R 1993, Large-scale crustal structure of the northwestern Yilgarn Craton, Western Australia: Evidence from Nd isotopic data and zircon geochronology: Tectonics, v. 12, p. 971–981.

Pawley, MJ, Wingate, MTD, Kirkland, CL, Wyche, S, Hall, CE, Romano, SS and Doublier, MP 2012, Adding pieces to the puzzle: Episodic crustal growth and a new terrane in the northeast Yilgarn Craton, Western Australia: Australian Journal of Earth Sciences, v. 59, no. 5, p. 603–623.

Perring, CS, Barnes, SJ and Hill, RET 1995, The physical volcanology of Archaean komatiite successions from Forrestania, Southern Cross Province, Western Australia: Lithos, v. 34, no. 1–3, p. 189–207.

Pidgeon, RT 1994, Investigation of the age and rate of deposition of part of the Gossan Hill Group, Golden Grove using conventional single grain zircon U–Pb geochronology: Geological Society of Australia, 12th Australian Geological Convention Abstracts, Perth.

Pidgeon, RT and Hallberg, JA 2000, Age relationships in supracrustal successions of the northen part of the Murchison Terrane, Archaean Yilgarn Craton, Western Australia: A combined field and zircon U-Pb study: Australian Journal of Earth Sciences, v. 47, p. 153–165.

Pidgeon, RT and Wilde, SA 1990, The distribution of 3.0 Ga and 2.7 Ga volcanic episodes in the Yilgarn craton of Western Australia: Precambrian Research, v. 48, p. 309–325.

Pidgeon, RT, Furfaro, D and Clifford, BA 1994, Investigation of the age and rate of deposition of part of the Gossan Hill Group, Golden Grove using conventional single grain zircon U–Pb geochronology, in Abstracts: Twelfth Australian Geological Convention-Geoscience Australia — 1994 and Beyond, Perth: Geological Society of Australia, p. 346.

Pidgeon, RT, Wilde, SA, Compston, W and Shield, MW 1990, Archaean evolution of the Wongan Hills greenstone belt, Yilgarn Craton, Western Australia: Australian Journal of Earth Sciences, v. 37, p. 279–292.

Polat, A, Appel, PWU, Fryer, B, Windley, B, Frei, R, Samson, IM and Huang,

H 2009, Trace element systematics of the Neoarchean Fiskenæsset anorthosite complex and associated meta-volcanic rocks, SW Greenland: Evidence for a magmatic arc origin: Precambrian Research, v. 175, no. 1–4, p. 87–115.

Polat, A, Frei, R, Scherstén, A and Appel, PWU 2010, New age (ca. 2970Ma), mantle source composition and geodynamic constraints on the Archean Fiskenæsset anorthosite complex, SW Greenland: Chemical Geology, v. 277, no. 1–2, p. 1–20.

Puchtel, IS, Hofmann, AW, Amelin, YV, Garbe-Schönberg, D, Samsonov, AV and Shchipansky, AA 1999, Combined mantle plume-island arc model for the formation of the 2.9 ga sumozero-kenozero greenstone belt, se Baltic Shield: isotope and trace element constraints: Geochimica et Cosmochimica Acta, v. 63, p. 3579–3595.

Pyke, J 2000, Minerals laboratory staff develops ICP-MS preparation method: Australian Geological Survey Organisation Newsletter, v. 33, p. 12–14.

Qiu YM, McNaughton NJ, Groves DI and Dalstra HJ 1999, Ages of internal granitoids in the Southern Cross region, Yilgarn Craton, Western Australia, and their crustal evolution and tectonic implications. Australian Journal of Earth Sciences, v. 46, p. 971–981.

Quentin de Gromard, R, Ivanic, TJ and Zibra, I 2021, Pre-Mesozoic interpreted bedrock geology of the southwest Yilgarn, *in* Accelerated Geoscience Program extended abstracts *compiled by* Geological Survey of Western Australia: Geological Survey of Western Australia Record 2021/4, p. 122–144.

Romano, SS, Thébaud, N, Mole, DR, Wingate, MTD, Kirkland, CL and Doublier, MP 2014, Geochronological constraints on nickel metallogeny in the Lake Johnston belt, Southern Cross Domain: Australian Journal of Earth Sciences, v. 61, no. 1, p. 143–157.

Schiøtte, L and Campbell, IH 1996, Chronology of the Mount Magnet granite-greenstone terrain, Yilgarn Craton, Western Australia: Implications for field-based predictions of the relative timing of granitoid emplacement: Precambrian Research, v. 78, p. 237–260.

Sharpe, R and Gemmell, JB 2001, Alteration characteristics of the Archean Golden Grove Formation at the Gossan Hill deposit, Western Australia: Induration as a focusing mechanism for mineralizing hydrothermal fluids: Economic Geology, v. 96, no. 5, p. 1239–1262.

Sharpe, R and Gemmell, JB 2002, The Archean Cu-Zn magnetite-rich Gossan Hill volcanic-hosted massive sulfide deposit, Western Australia: Genesis of a multistage hydrothermal system: Economic Geology, v. 97, no. 3, p. 517–539.

Smithies, RH, Champion, DC, Van Kranendonk, MJ, Howard, HM and Hickman, AH 2005, Modern-style subduction processes in the Mesoarchaean: Geochemical evidence from the 3.12 Ga Whundo intra-oceanic arc: Earth and Planetary Science Letters, v. 231, no. 3–4, p. 221–237.

Smithies, RH, Ivanic, TJ, Lowrey, JR, Morris, PA, Barnes, SJ, Wyche, S and Lu, Y-J 2018a, Two distinct origins for Archean greenstone belts: Earth and Planetary Science Letters, v. 487, p. 106–116.

Smithies, RH, Lu, Y, Gessner, K, Wingate, MTD and Champion, DC 2018b, Geochemistry of Archean granitic rocks in the South West Terrane of the Yilgarn Craton: Geological Survey of Western Australia, Record 2018/10, 13p.

Söderlund, U, Patchett, PJ, Vervoort, JD and Isachsen, CE 2004, The 176Lu decay constant determined by Lu–Hf and U–Pb isotope systematics of Precambrian mafic intrusions: Earth and Planetary Science Letters, v. 219, no. 3, p. 311–324.

Stacey, JS and Kramers, JD 1975, Approximation of terrestrial lead isotope evolution by a two-stage model: Earth and Planetary Science Letters, v. 26, p. 207–221.

Steiger, RH and Jäger, E 1977, Subcommission on geochronology: Convention on the use of decay constants in geo- and cosmochronology: Earth and Planetary Science Letters, v. 36, p. 359–362.

Stern, RA, Bodorkos, S, Kamo, SL, Hickman, AH and Corfu, F 2009, Measurement of SIMS instrumental mass fractionation of Pb isotopes during zircon dating: Geostandards and Geoanalytical Research, v. 33, p. 145–168.

Thebaud, N, Mole, DM, Wingate, MTD, Kirkland, CL and Doublier, MP 2013a, 205916: metasyenogranite, Withers Find Road; Geochronology Record 1121: Geological Survey of Western Australia, 5p.

Thebaud, N, Wingate, MTD, Kirkland, CL and Doublier, MP 2013b, 205912: granodiorite gneiss, Lake Julia; Geochronology Record 1114: Geological Survey of Western Australia, 5p.

Thern, ER, Jourdan, F, Evans, NJ, McDonald, B, Danisik, M, Frew, R and Nelson, DR 2011, Post-depositional thermal history of the 4364–3060 Ma zircon-bearing: Mineralogical Magazine, Goldschmidt Conference Abstracts, p. 2003.

Thern, ER, and Nelson, DR 2012, Detrital zircon age structure within ca 3 Ga metasedimentary rocks, Yilgarn craton: Elucidation of Hadean source terranes by principal component analysis: Precambrian Research, v. 214, p. 28–43.

Thern, ER, Blereau, E, Jourdan, F, Nelson, DR, 2020 Tourmaline $^{40}Ar/^{39}Ar$ geochronology and thermochronology: Example from Hadean-zircon-bearing siliciclastic metasedimentary rocks from the Yilgarn Craton, Geochimica et Cosmochimica Acta, 277, p285–299. https://doi.org/10.1016/j.gca.2020.03.008

Van Kranendonk, MJ, Ivanic, TJ, Wingate, MTD, Kirkland, CL and Wyche, S 2013, Long-lived, autochthonous development of the Archean Murchison Domain, and implications for Yilgarn Craton tectonics: Precambrian Research, v. 229, p. 49–92.

Wang, Q 1998, Geochronology of the granite-greenstone terranes in the Murchison and Southern Cross Provinces of the Yilgarn Craton, Western Australia: Australian National University, Canberra, PhD thesis (unpublished), 186p.

Wang, Q, Campbell, IH and Schiøtte, L 1996, Geochronological constraints on the age of komatiites and nickel mineralisation in the Lake Johnston greenstone belt, Yilgarn Craton, Western Australia: Australian Journal of Earth Sciences, v. 43, p. 381–385.

Wang, Q, Schiøtte, L and Campbell, IH 1998, Geochronology of supracrustal rocks from the Golden Grove area, Murchison Province, Yilgarn Craton, Western Australia: Australian Journal of Earth Sciences, v. 45, p. 571–577.

Wang, Q, Beeson, J and Campbell, IH 1998, Granite-greenstone zircon U-Pb chronology of the Gum Creek greenstone belt, Southern Cross Province, Yilgarn Craton: Tectonic implications, *in* Structure and evolution of the Australian continent *edited by* J Braun, J Braun, J Dooley, J Dooley, BR Goleby, BR Goleby, R van der Hilst, R van der Hilst, C Klootwijk and C Klootwijk: American Geophysical Union, Geodynamics series, p. 175–186.

Watkins, KP and Hickman, AH 1990, Geological evolution and mineralization of the Murchison Province, Western Australia: Geological Survey of Western Australia, Bulletin 137, 267p.

Wilde, SA, Middleton, MF and Evans, BJ 1996, Terrane accretion in the southwestern Yilgarn Craton: Evidence from a deep seismic crustal profile: Precambrian Research, v. 78, p. 179–196.

Wingate, MTD, Bodorkos, S and Kirkland, CL 2008a, 184112: metasandstone, Ram Well; Geochronology Record 736: Geological Survey of Western Australia, 6p.

Wingate, MTD, Bodorkos, S and Kirkland, CL 2008b, 177904: quartzite, Windmill Hill; Geochronology Record 740: Geological Survey of Western Australia, 7p.

Wingate, MTD, Kirkland, CL and Hall, CE 2010, 193363: metadacite, Lake Wells Homestead; Geochronology Record 927: Geological Survey of Western Australia, 4p.

Wingate, MTD, Kirkland, CL and Hall, CE 2011a, 185979: fine-grained quartzite, Lake Wells Homestead; Geochronology Record 955: Geological Survey of Western Australia, 5p.

Wingate, MTD, Kirkland, CL and Pawley, MJ 2011b, 179448: biotite tonalite, Mount Cumming; Geochronology Record 945: Geological Survey of Western Australia, 4p.

Wingate, MTD, Kirkland, CL and Hickman, AH 2012a, 178165: metagabbro, Munni Munni Creek; Geochronology Record 1071: Geological Survey of Western Australia, 4p.

Wingate, MTD, Kirkland, CL and Ivanic, TJ 2012b, 193972: metarhyolite clast in volcaniclastic breccia, Weld Range; Geochronology Record 1011: Geological Survey of Western Australia, 4p.

Wingate, MTD, Kirkland, CL, Van Kranendonk, MJ and Wyche, S 2013, 155569: metarhyolite, Weld Range; Geochronology Record 1096: Geological Survey of Western Australia, 4p.

Wingate, MTD, Kirkland, CL and Ivanic, TJ 2015a, 198213: syenogranite gneiss, Dixon Bore; Geochronology Record 1233: Geological Survey of Western Australia, 4p.

Wingate, MTD, Kirkland, CL and Ivanic, TJ 2015b, 198240: felsic metavolcanic breccia, Weld Range; Geochronology Record 1235: Geological Survey of Western Australia, 4p.

Wingate, MTD, Kirkland, CL and Zibra, I 2015c, 155879: granodiorite gneiss, Toben Bore; Geochronology Record 1245: Geological Survey of Western Australia, 4p.

Wingate, MTD and Lu, Y 2017, Introduction to geochronology information released in 2017: Geological Survey of Western Australia, 5p.

Wingate, MTD, Lu, Y, Kirkland, CL and Romano, SS 2017a, 207514: felsic metavolcanic rock, Maggie Hays mine; Geochronology Record 1412: Geological Survey of Western Australia, 4p.

Wingate, MTD, Lu, Y, Kirkland, CL and Romano, SS 2017b, 207517: felsic metavolcanic rock, Round Top Hill; Geochronology Record 1435: Geological Survey of Western Australia, 4p.

Wingate, MTD, Lu, Y, Kirkland, CL and Romano, SS 2017c, 207513: felsic metavolcanic rock, Maggie Hays mine; Geochronology Record 1411: Geological Survey of Western Australia, 3p.

Wingate, MTD, Lu, Y, Kirkland, CL and Romano, SS 2017d, 207506: quartzite, Overshot Hill; Geochronology Record 1368: Geological Survey of Western Australia, 4p.

Wingate, MTD, Lu, Y and Romano, SS 2018a, 207510: metatonalite, Mount Chester; Geochronology Record 1459: Geological Survey of Western Australia, 4p.

Wingate, MTD, Outhwaite, MD and Lu, Y 2018b, 205930: monzogranite gneiss, Dasher Prospect; Geochronology Record 1455: Geological Survey of Western Australia, 5p.

Wingate, MTD, Outhwaite, MD and Lu, Y 2018c, 205931: syenogranitic gneiss, Dasher prospect; Geochronology Record 1456: Geological Survey of Western Australia, 4p.

Wingate, MTD, Lu, Y and Ivanic, TJ 2019, 207670: felsic metavolcaniclastic rock, Morawa–Yalgoo Road; Geochronology Record 1578: Geological Survey of Western Australia, 4p.

Wingate, MTD, Lu, Y and Zibra, I 2020, 219311: metamonzogranite, North Paradise Well; Geochronology Record 1680: Geological Survey of Western Australia, 4p.

Wingate, MTD, Fielding, IOH, Lu, Y and Ivanic, TJ 2021a, 242405: metamonzogranite, Mount Gibson mine; Geochronology Record 1805: Geological Survey of Western Australia, 4p.

Wingate, MTD, Fielding, IOH, Lu, Y and Ivanic, TJ 2021b, 242407: metadacite, Bungeye Well; Geochronology Record 1806: Geological Survey of Western Australia, 4p.

Wingate, MTD, Fielding, IOH, Lu, Y and Ivanic, TJ 2021c, 227224: tonalite, Edamurta Range; Geochronology Record 1803: Geological Survey of Western Australia, 4p.

Witt, WK 1998, Geology and mineral resources of the Ravensthorpe and Cocanarup 1:100 000 sheets: Geological Survey of Western Australia, Report 54, 152p.

Witt, WK 1999, The Archaean Ravensthorpe Terrane, Western Australia: Synvolcanic Cu-Au mineralization in a deformed island arc complex: Precambrian Research, v. 96, no. 3-4, p. 143–181.

Woodhead, JD and Hergt, JM 2005, A preliminary appraisal of seven natural zircon reference materials for in situ Hf isotope determination: Geostandards and Geoanalytical Research, v. 29, p. 183–195

Wyche, S 2007, Evidence of pre-3100 Ma crust in the Youanmi and South West Terranes, and Eastern Goldfields Superterrane, of the Yilgarn Craton, in Earth's Oldest Rocks *edited by* MJ Van Kranendonk, RH Smithies and VC Bennett: Elsevier BV, Burlingtion, Massachusetts, Developments in Precambrian Geology 15, p. 113–123.

Wyche, S, Kirkland, CL, Riganti, A, Pawley, MJ, Belousova, E and Wingate, MTD 2012, Isotopic constraints on stratigraphy in the central and eastern Yilgarn Craton, Western Australia: Australian Journal of Earth Sciences, v. 59, no. 5, p. 657–670, doi:10.1080/08120099.2012.697677.

Wyche, S, Nelson, DR and Riganti, A 2004, 4350-3130 Ma detrital zircons in the Southern Cross Granite-Greenstone Terrane, Western Australia: Implications for the early evolution of the Yilgarn Craton: Australian Journal of Earth Sciences, v. 51, p. 31–45.

Yeats, CJ, McNaughton, NJ and Groves, DI 1996, SHRIMP U-Pb geochronological constraints on Archean volcanic-hosted massive sulfide and lode gold mineralization at Mount Gibson, Yilgarn Craton, Western Australia: Economic Geology, v. 91, no. 8, p. 1354–1371.

Zibra, I, Ivanic, TJ, Chen, SF, Clos, F, Li, J, Gu, P, Meng, Y and Wang, C 2016, Badja, WA Sheet 2240: Geological Survey of Western Australia, 1:100 000 Geological Series.

Zibra, I, Ivanic, TJ, Chen, SF, Clos, F, Li, J, Gu, P, Meng, Y and Wang, C 2017, Thundelarra, WA Sheet 2340: Geological Survey of Western Australia, 1:100 000 Geological Series.

Zibra, I, Lu, Y, Clos, F, Weinberg, RF, Peternell, M, Wingate, MTD, Prause, M, Schiller, M and Tilhac, R 2020, Regional-scale polydiapirism predating the Neoarchean Yilgarn Orogeny: Tectonophysics, v. 779, p. 228375, doi:10.1016/j.tecto.2020.228375.

Zibra, I, Peternell, M, Schiller, M, Wingate, MTD, Lu, Y and Clos, F 2018, Tectono-magmatic evolution of the Neoarchean Yalgoo dome (Yilgarn Craton): diapirism in a pre-orogenic setting: Geological Survey of Western Australia, Report 176, 43p.

REPORT
232

FORMATION OF THE YILGARN PROTOCRATON BY RIFT-RELATED MAGMATISM FROM 3.01 TO 2.92 GA

TJ Ivanic, MTD Wingate, JR Lowrey and Y Lu

New geochronology from across the western Yilgarn Craton demarcates, in time and space, a 100 Ma period of extensive but sporadic magmatism followed by 100 Ma of quiescence. By 2920 Ma, abundant new crust had been added to what we suggest was a coherent Yilgarn protocraton that would remain relatively untouched until 2825 Ma, with deposition of the Norie Group. We describe the stratigraphic–magmatic framework of several volcano-sedimentary greenstone belts and granitic suites in the Youanmi Terrane from 3018 Ma to 2920 Ma and suggest a rift tectonic setting in light of new Hf isotopic data. We named the greenstones and granites of this time interval the Southern Cross Supergroup and Thundelarra Supersuite. Although our results shed light on these, much further work is required for a thorough understanding of these significant geological units.

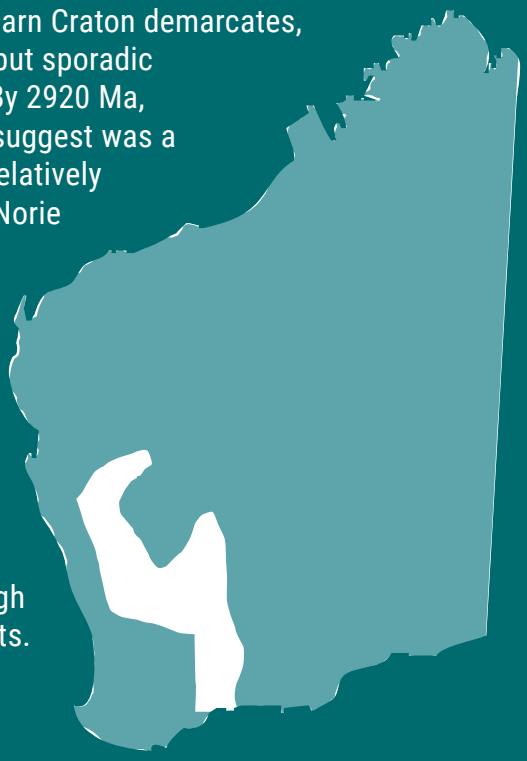

Further details of geoscience products are available from:

First Floor Counter
Department of Mines, Industry Regulation and Safety
100 Plain Street
EAST PERTH WESTERN AUSTRALIA 6004
Phone: +61 8 9222 3459 Email: publications@dmirs.wa.gov.au
www.dmirs.wa.gov.au/GSWApublications